U.S. DEPARTMENT OF THE INTERIOR

U.S. GEOLOGICAL SURVEY

PRELIMINARY EVALUATION OF RECENT MOVEMENT ON STRUCTURES WITHIN THE SANTA MONICA BASIN, OFFSHORE SOUTHERN CALIFORNIA

By

William R. Normark[1] and David J.W. Piper[2]

Open-File Report 98-518

Prepared in cooperation with the
Geological Survey of Canada

1998

1. Menlo Park, California 94025
2. Geological Survey of Canada (Atlantic); Dartmouth, Nova Scotia; Canada

ABSTRACT

A joint study by the Geological Survey of Canada and U.S. Geological Survey of the submarine turbidite systems formed in the Santa Monica Basin of the California continental borderland provides limited observation of previously mapped fault systems generally associated with the basin margins. This report evaluates the use of high-resolution seismic-reflection data, primarily from a deep-towed boomer system, to determine the character of deformation and to evaluate the timing of the most recent activity. The ages of key reflectors that have been mapped across much of the basin floor are established through correlation with dated cores from Ocean Drilling Program Site 1015. In general, the deep-tow boomer records show that deformation within the last 20 ky is common: (1) along traces of the San Pedro Basin fault zone within the northeast margin of the basin and (2) in the western corner of the Santa Monica Basin near the intersection of northwest-trending faults interpreted to experience oblique slip with east-west-trending structures associated with compression within the Transverse Ranges. Locally, fault displacement in these two areas offsets the sea floor or reaches within a few meters of the sea floor. Deeper penetration seismic-reflection profiles obtained during the same study indicate deformation elsewhere along basin-margin faults during the last 70 ky.

INTRODUCTION

The California continental borderland, which constitutes part of the distributed, tectonically active boundary between the Pacific and North American plates, bounds the western side of the most populous urban corridor in the western U.S. (Fig. 1). Destructive earthquakes are common within this broad plate boundary, e.g. the 1994 Northridge earthquake (M_w6.7) is the most recent to cause major devastation. Over the last several decades, tectonic syntheses for the Borderland have identified the general distribution of the offshore (and related onshore) fault systems (Clarke et al., 1985; Greene and Kennedy, 1986; Vedder, 1987; Wallace, 1990; Legg, 1991; Crouch and Suppe, 1993; Clarke and Kennedy, 1997; Bohannon and Geist, 1998). Although the general fault pattern has been recognized, the deformation character, history of displacement, and significance relative to the overall seismic hazard for the region are poorly known for faults within the offshore area.

The continental shelf and inner borderland basins are sites of relatively rapid accumulation of terrigenous sediment (see summaries by Nardin, 1983; Schwalbach and Gorsline, 1985; Shipboard Scientific Party, 1997; Normark et al., 1998). Characterization of the deformation of sediment fill in the inner borderland basins can provide a method to evaluate the hazard potential of large, destructive earthquakes and indicate how the seismic risk is distributed with respect to the adjacent Southern California metropolitan centers. In this study, we look for deformation of the turbidite-sediment fill of submarine fans and coeval basin-slope sediment to determine the character and history of deformation within the offshore Santa Monica Basin during the last 40 to 70 ka.

The approach in this report is to document the evidence for and age of deformation of the turbidite and slope deposits in the vicinity of the previously mapped faults within the Santa Monica Basin (Figs. 2 and 3). A primary purpose of this report is to evaluate the use of the Huntec deep-tow boomer system to provide high-resolution stratigraphic control that

can be tied to dated core samples to establish the timing of deformation. Although the new data suggest a revaluation of the fault pattern in Santa Monica Basin is necessary, there is, at this time, insufficient coverage to justify redrawing the generalized fault pattern as depicted in Figure 3. This work is further preliminary in nature pending both the collection of additional high-resolution seismic-reflection data and improved chronology for the sediment cored at ODP Site 1015 (Lyle, personal communication, 1998).

BACKGROUND

This study is based on data available from a detailed seismic-reflection investigation in early 1992 of the Hueneme fan and related turbidite systems in the western half of Santa Monica Basin (Fig. 2). The survey, which was a cooperative activity conducted by the Geological Survey of Canada (GSC) and the U.S. Geological Survey (USGS), was designed to determine the seismic-stratigraphy and architectural elements (*sensu* Mutti and Normark, 1987) of the turbidite systems that are filling Santa Monica Basin (Piper et al., 1995; Normark et al., 1998: Piper et al., in press). During the survey, the lowermost parts of the basin slopes, principally on the northern and southwestern sides of Santa Monica Basin, were traversed by several of the survey lines; these data provide an opportunity to evaluate the style of deformation along the basin margins but are insufficient to justify remapping the fault pattern.

Figure 3 provides a schematic compilation of the fault systems in Santa Monica Basin that have been identified during previous studies, primarily by Clarke et al. (1985), Greene and Kennedy (1986), Vedder (1987), Legg (1991), and Crouch and Suppe (1993). The northeast and southwest margins of the basin are marked by systems of parallel to subparallel faults locally associated with steep basin slopes. There is a marked change in structural character along the northern margin of Santa Monica Basin near 34°N Lat. from northwesterly to east-west trending faults. Much of the deformation south of 34°N Lat. is associated with strike-slip or oblique-slip fault movement whereas folding and thrusting dominate the deformation north of 34°N. Lat. (Clarke et al., 1985; Klitgord and Brocher, 1996). Within the main grid of survey tracklines on the floor of the basin, the earlier studies have identified few fault systems (Figs. 2 and 3). The turbidite systems, which include the Hueneme and Dume submarine fans (Figs. 3 and 4), are fed from submarine canyons that cross the east-west trending faults along the northern margin of the basin. On the floor of Santa Monica Basin, these fan deposits apparently are underlain only by short fault segments that have a trend intermediate to fault systems that bound the basin (Fig. 3; K. Klitgord, written comm., 1997).

METHODOLOGY

There are two components to this study. The first involves definition of a seismic-stratigraphic framework that can be used to interpret depositional geometry within the sediment fill of Santa Monica Basin and to distinguish between structural and depositional relief that affects the sea floor and subbottom reflectors. It should be possible to establish time-correlative events in different areas to the extent that key reflectors within the stratigraphic framework can be mapped throughout the basin. Normark et al. (1998) and Piper et al. (in press) developed a seismic-stratigraphic framework for the submarine fans in Santa Monica Basin and identified 15 key reflectors, some of which can be traced

across much of the basin (Fig. 4). These key reflectors are denoted in alphabetical order from the deepest (A) to the shallowest (O); no additional stratigraphic markers were identified in this current study. In this report, we examine what happens to these 15 key reflectors along the basin margins, where most of the fault systems have been found, seeking evidence for non-depositional relief or discontinuities within the turbidite and slope sediment.

The second component of the study involves assigning ages to the key stratigraphic reflectors to determine the timing and extent of deformation within the basin-fill sequences. The ages of reflectors can be determined by extrapolation of sedimentation rates determined from surficial sediment cores (standard box, gravity, and piston cores) from throughout the basin (see compilation of Nardin, 1981, 1983) and by correlation with the deeper sequences recovered at ODP Site 1015 (Shipboard Scientific Party, 1997).

Seismic-reflection systems

Collection of the seismic-reflection data for this study utilized three systems with differing reflector resolution and acoustic-penetration capabilities. For conventional seismic-reflection profiling, a Texas Instruments 40 cu-in (650 cm^3) sleeve gun, run at 1300 psi, was fired every 3 s. Signals were detected on a Seismic Engineering (SE) 30-m hydrophone array and a Nova Scotia Research Foundation (NSRF) Mark 5a 6-m hydrophone array. The 30-m SE streamer provided good data typically to depths of about 1 s (800 to 1000 m) with reflector resolution of about 10 ms round-trip travel (~ 8 m assuming a sound velocity of 1500 m/s) (Fig. 5a). The NSRF array obtained useful data to about 0.4 s subbottom, but with a higher frequency bandwidth that provided resolution of about 5 ms (~ 3 m) (Fig. 5b).

In addition, a high-resolution Huntec DTS boomer system towed several hundred meters below the sea surface (about a third the water depth) was used to image the upper few tens of milliseconds of strata with a resolution of better than 0.5 ms (0.4 m) (Fig. 5c). Power output was 540 Joules with a firing rate of 0.75 sec, and returning signals were received by a 5-m-long Benthos 10-element hydrophone array. Signals were filtered at 500-6000 Hz and recorded at a 0.25 sec sweep. The survey speed of 5 kt (9.25 km/hr) resulted in a shot spacing of less than 2 m for the deep-tow boomer profiles.

The survey tracklines (Fig. 2) are accurate to ± 30 m based on GPS data. The position data for structures observed in this study are more accurate than that for some earlier (10 to 15 years ago) surveys, which have provided the basis for the fault pattern depicted in Figure 3. Some structures illustrated using our survey data do not align with the mapped structures depicted in Figure 3, but there are insufficient new data at this time to remap fault locations.

Figure 5 illustrates the characteristics of output along the same trackline from the three seismic-reflection systems used for mapping structural features in Santa Monica Basin. The profiles along this track cross the southwestern basin margin at the base of a relatively steep slope (Figs. 2 and 3). Figure 5A shows folding of the basin fill is more pronounced with depth and only gentle upwarp of the basin fill is observed by the time of reflectors J and F. There is a suggestion of a faulted contact between the deeper basin margin and sediment fill below about 200 m. Figure 5B, in contrast, shows distinct tilting with an unconformity at reflector J time. Only with the higher resolution of the deep-tow

boomer data, however, is uplift and tilting of the basin sediment observed at the base of the slope (Fig. 5C).

In general, structural deformation is recognized in several ways. In the 30-m SE and NSRF profiles, abrupt offsets in subparallel reflections appear to mark faults. These offsets commonly are associated with low-dip anticlines. Similar features are visible in the Huntec profiles, but the greater resolution allows recognition of more subtle folding or tilting in strata close to fault surfaces. In addition, the Huntec profiles show acoustically incoherent features that might be related to fluid escape.

Sediment data and chronology

Large numbers of box cores and fewer short piston cores from the Santa Monica Basin have been described by Gorsline and Emery (1959), Reynolds (1987), Gorsline (1996) and Edwards et al. (1996). Nardin (1981, 1983) compiled available age data from these cores to suggest that a prominent reflector at about 8 m subbottom in his 3.5-kHz profiles from Santa Monica Basin (approximately equivalent to reflector N of Normark et al., 1998) has an age of about 10 ka (sedimentation rate of about 0.8 m/ka).

Chronology for late Quaternary sediment in Santa Monica Basin is based on ^{210}Pb chronology from box core samples (Christensen et al., 1994). Gorsline (1996) used this technique to identify a 0.56 ka turbidite over large areas of the lower fan in 40-50 cm long box cores, implying accumulation rates of ~1 m/ka. Correlation with ODP Site 1015 (Figs. 2 and 3) provides chronology for deeper sequences (Shipboard Scientific Party, 1997). The deepest sediment recovered from Site 1015 at 150 mbsf (meters below sea floor) is <60 ka. Comparison of foraminiferal assemblages from Site 1015 (Shipboard Scientific Party, 1997, p. 228) with the succession in ODP Site 893 in nearby Santa Barbara Basin (Fig. 1; Shorebased Scientific Party, 1994), where there is a well-dated biostratigraphy (Kennett and Venz, 1995), suggests the following correlations for Site 1015 in Santa Monica Basin:

Depth (mbsf)	Age (ka)	Key indicators
26	15	Common *G. bulloides*; few *N. pachyderma* (dex); common *G. inflata*
64-74	18	Peak in *N. pachyderma* (dex), absent below; start of abundant *N. pachyderma* (sin)
140-150	30-35	Some *N. pachyderma* (dex); common, then absent *N. pachyderma* (sin); common *G. bulloides*

These three correlations result in reasonable estimates of the sedimentation rate for the uppermost basin fill. Rates are about 1 m /ka in most of the Holocene and 2-4 m/ka during the late Pleistocene. More robust correlations should be available when oxygen isotopic data from Site 1015 are published.

Subbottom depths of key reflectors from Normark et al. (1998) can be projected to Site 1015 from the closest approaches of the survey lines that enclose the site; the closest lines pass about 5 km south and 9 km north of the site (Figs. 2 and 3). Piper et al. (in

press) present a detailed seismic stratigraphy for the flat-lying sediment of the basin plain that can be recognized in both the line to the north and the line to the south of the site (see their Figure 10). These key reflectors can be projected into Site 1015 with an uncertainty of less than +/- 1 ms. The depths to key reflectors, measured in round-trip travel time, are converted to depths using a sound velocity of 1500 m/s at the sea floor to almost 1600 m/s at the bottom of the hole based on correlation of key reflector spacing with the bulk density profile for the cores at Site 1015 (Shipboard Scientific Party, 1997). Errors in age estimates resulting from seismic correlation are less than +/- 500 yr; errors associated with the preliminary age picks from Site 1015 are probably +/- 1 ka for ages less than 20 ka and rather more for the older ages. Throughout this report, ages are based on the assignments presented in Table 1 extrapolated using the assumption of uniform sedimentation rates.

RESULTS

Displacement on fault systems in Santa Monica Basin falls within three groups: (1) east-west structures parallel to the faults within the Transverse Ranges along the northern margin of Santa Monica Basin; (2) northwest-southeast structures that generally parallel the San Andreas fault system reflecting the orientation of the Pacific-North American plate boundary; faults of this trend include those along the southwest and northeast margins of the Santa Monica Basin; and (3) west-northwest/east-southeast structures with trends intermediate between (1) and (2); faults with WNW/ESE trends are found only in the northern part of Santa Monica Basin south of the Transverse-Range parallel structures (Fig. 3). These groupings of fault trends are discussed in a generally clockwise order beginning with the east-west faults at the northern margin of the basin.

E-W structures parallel to Transverse Range faults

Only one fault trending east-west was crossed during the survey along the northern edge of the basin (see survey grid in the area between 119° 00' and 119° 10' Long.; Figs. 2 and 3). This east-west fault is probably the eastern continuation of the Santa Cruz Island fault that is variously identified as the Anacapa fault (Clarke et al., 1985), Anacapa-Dume fault (Dolan et al., 1997), and Dume fault (Pinter et al., 1998). The northern margin of the Santa Monica Basin involves some of the greatest relief on the Hueneme fan, and the location of the fault is uncertain along the northern edge of the fan (Fig. 3). Unequivocal evidence for structural disturbance involving the turbidite marker horizons within the fan sequence is difficult to identify along this edge of the fan, where erosion from turbidity currents as well as mass wasting are common (Normark et al., 1998; Piper et al., in press). The steep basin margin between Mugu and Dume canyons (Fig. 2), which is observed only as hyperbolic reflections in all seismic records, is the best evidence for a major active fault. The eastward continuation of this inferred fault lies outside (north of) all our seismic tracks east of longitude 119º 08'W (Figs. 2 and 3).

One seismic-reflection profile on the northwestern part of the fan (Fig. 6A) crosses the westward projection of the fault along the northern basin margin and shows apparent fault offsets in bedrock or deformed sediment. One possible fault extends upward to below key reflector A and two others to reflector C, but overlying sediment appears to be depositionally continuous. Apparent breaks in reflector continuity in the upper 100 m of

sediment imaged with the NSRF streamer may have a sedimentological origin; Huntec data are not available for this section.

On the eastern side of Hueneme Fan, a series of small faults cut deep strata below reflector A (Fig. 6B) and may extend to near surface. Huntec profiles (not illustrated) show apparent 2 m offsets of strata at 15 m subbottom depth and apparent vertical fluid escape features above the southernmost deep fault illustrated in Figure 6B.

A Huntec profile (Fig. 6C) located about 10 km east of the profile in Figure 6B and about 500 m south of the hyperbolic echoes from the main fault-line scarp shows near-surface offsets of a few meters. In the NSRF records (not illustrated), the offsets are not evident and the underlying strata appear to be continuous. It is possible that the observed fault (Fig. 6C) results from syn-sedimentary instability with a component of bedding plane slip (perhaps triggered by local seismicity) rather than from upward propagation of a deep-seated tectonic fault.

On Hueneme fan, reflector offsets observed in the upper 50 m of sediment, which is well-imaged on Huntec profiles, are generally more consistent with erosion by turbidity currents or submarine slides. The deeper penetration 30-m SE and NSRF records show onlap of several hundred meters of sediment on the basin slope, below which there is some suggestion of fault control of the slope itself (Fig. 6A, 6B).

WNW-ESE 'intermediate' structures

Three transects from our 1992 geophysical survey cross the trends of two short curvilinear, subparallel faults at or near the base of the slope south of Point Dume (Figs. 7 and 8). The seismic-reflection records from the two slope-normal tracklines south-southwest of Point Dume (see inset Fig. 7) show no evidence for disruption of the near-surface sediment where the profiles cross the western extension of these intermediate trending faults. In this area, sediment from the Hueneme fan onlaps the coarser, more steeply dipping sediment of the Dume fan (Fig. 4, Line 57). The sleeve-gun 30-m SE profiles suggest faulting of the deeper basin slope, below about 300 ms (>225 m subbottom).

The easternmost survey transect that crosses the WNW-ESE fault segments shows evidence for more recent structural deformation (Fig. 7). The profile in Figure 7 shows many possible fault strands both on the mid slope and along the paleoslope-basin margin that are not indicated in Figure 3. All three seismic-reflection systems show evidence for faults that are buried but that coincide with the topographic break at the base of the slope. A more southerly set of faults occurs at the base of the paleoslope about the time of key reflector C (Fig. 7). To the south of the present edge of the basin floor, an anticline is offset by several reverse faults. The crest of the anticline lies at a subbottom depth of about 80 m (Fig. 7) and growth of the anticline has continued during deposition of the basin plain turbidites, affecting sediment at least as young as key reflector C (33 ka). All these faults have relatively shallow dips to the south and some appear to show reverse movement. On the Huntec profile, the fault closest to the present break in slope extends to within about 20 m of the surface and its upper limit might be obscured by a small slide mass (Fig. 8). The youngest beds affected by faulting are between key reflectors J and L, suggesting the last offset is about 15 ka (Table 1).

NW-SE structures on northeast flank of Santa Monica Basin

The San Pedro Basin fault zone (Ziony and Yerkes, 1985) parallels the Santa Monica Basin slope west of the Palos Verdes Peninsula together with several subparallel faults located farther basinward (Fig. 3). There is clear evidence for faulting from all three seismic-reflection systems on profiles that cross the mid-slope. The westernmost fault strands generally coincide with the walls of a submarine canyon and other gullies (Fig. 7), within which we were unable to determine the youngest sediment affected by displacement. The 30-m SE record suggests southwest-dipping faults with normal throw (Fig. 7).

A set of generally south-dipping faults disrupts the sediment that forms a small bench on the basin slope near the northeast end of Figure 7; the sense of offset on these strands is not uniform and might be affected by slumping related to the relief of the canyon immediately downslope (Figs. 7 and 9). The Huntec profile shows that two faults on the bench might extend to the sea floor, but there appears to be a thin unfaulted sediment drape that covers this part of the basin slope (Fig. 9). Toward the canyon (south), the sediment sequence cut by this fault is truncated basinward and covered by the same sediment drape (Fig. 9, southwest side).

Crossings of the San Pedro Basin fault zone farther southeast have less clear evidence for recent movement (Fig. 10). The San Pedro Basin fault itself appears on the reflection profiles as a notch on the basin slope that has been covered by a thin drape of sediment (upslope-most fault shown in Fig. 10). There is no clear indication of sense of offset on this inferred fault and the thin sediment drape is an isolated deposit that cannot be tied to the key-reflector stratigraphy of the basin. A short distance downslope, a similar notch buried by a sediment apron might indicate a parallel strand of the San Pedro Basin fault zone (shown as SPBF? in Fig. 10).

There is no evidence for deformation in the surficial-sediment wedge that onlaps the base of the lower slope (denoted 'crossing 6' in Fig. 10), but both the NSRF and 30-m SE profiles show a relatively steep fault that forms the deeper part of the basin margin. Sediment onlapping the lower slope has buried the fault tip by about 100 m. The Huntec record for this fault transect shows no offset in the upper 50 m of sediment.

The westernmost fault strand on the lower slope (Fig. 3) roughly parallels the San Pedro Basin fault but appears to converge with it to the northwest. There is a pronounced piercement structure on this fault strand; basin turbidite sediment underlies both lower flanks of this structure (Figs. 10 and 11). Sediment on the flanks of this feature thins to about 70% of its thickness in adjacent flat-lying areas (Fig. 10). The faults bounding this structure (Figs. 10 and 11) are inferential because no offset strata are unequivocally matched in the "diapir"; a thick, asymmetric sediment fill is truncated on the both sides of this piercement structure.

Four kilometers south, on the north side of Redondo Knoll (Fig. 2), there is a zone of limited deformation (Fig. 12). Seismic stratigraphy in the southeasternmost end of the Santa Monica Basin plain is based on correlation by reflector character and thickness with the main part of the basin plain. In the NSRF profile (not illustrated), an asymmetrical anticline deforms sediment younger than J; the deformation extends through a section that is laterally equivalent to the section cut by the piercement structure shown in Figure 11. In

the Huntec profile (Fig. 12A), the upbowing of the turbidite basin-plain sequence clearly reaches as shallow as horizon L and probably to within two meters of the sea floor. On the steep (north) side of the anticline, a zone of disruption (lack of internal reflectors) on the Huntec profile may reflect faulting and/or the presence of fluids. At the margin of the basin plain a short distance south (Fig. 12B), some fault offset is visible at the base of the paleoslope about 40 m below the sea floor. A small slide mass just below horizon L appears to be at the same stratigraphic level as a slide seen farther northeast (Fig. 8) and might indicate a seismic event that affected slope-sediment stability throughout the eastern end of Santa Monica Basin.

NW-SE structures on southwest margin of Santa Monica Basin

The southwest margin of Santa Monica Basin is formed by a major northwest-trending fault zone that results in the steepest relief within the basin (Fig. 3). The deformation observed in the basin-fill turbidites along the southwest margin generally increases to the northwest, and the seismic-reflection data will be discussed from southeast to northwest.

Figure 5C suggests that sediment younger than key reflector N (10 - 11 ka) has been tilted and deeper reflectors possibly offset at the base of the slope. The deeper acoustic-penetration systems (Figs. 5A, B), however, show that deformation of the turbidite basin fill below key reflector F extends farther basinward. The deformation above about 200 m subbottom depth in the sediment is limited to gentle upwarping near the margin faults (Figs. 5A and B), but a gentle anticlinal structure at the basin margin shows possible fault offset of its southwestern flank. This flank of the basin is buried by a ~200-m-thick sequence of turbidites that show progressively less deformation upward (Fig. 5 A) except for gentle tilting toward the basin axis.

Deep-tow boomer profiles show more extensive deformation near the base of the slope closer to the northwestern corner of Santa Monica Basin (Fig. 13). Upward tilting of the outer Hueneme fan turbidite sequence (Normark et al., 1998) is similar to that observed in Figure 5, but here the hinge area near the base of slope involves mainly sediment below key reflector N. A depression (graben?) along the base of the slope is being filled with young turbidite deposits creating an unconformity (southern end of Fig. 13). Tilting of the turbidite fill (identified as such by its planar bedding and reflector character) in this slope-base depression suggests relatively recent movement. The total offset associated with the depression could not be determined with our data.

A short distance north of the Holocene tilting and unconformity noted in Figure 13 and described above, a broad area of folded basin-fill turbidites is present near the base of the slope. Figures 14A and B, which comprise a U-shaped transect, show that anticlinal folds are developed near the slope. Sediment farther basinward shows the gentle upwarping similar to that observed further southeast (c.f. Figs. 12 and 13). The north-south segment of Figure 14A shows that flanks of the anticlines are cut by faults. The folding and faulting, which is most pronounced for sediment below key reflector J, apparently has not affected the youngest fan sediment except for the gentle tilt toward the basin (west side in Fig. 14B). The Huntec record along the profile of Figure 14 suggests that there has been no deformation of sediment younger than key reflector M, which might involve subtle upbowing that is difficult to distinguish from depositional relief.

At the northwestern corner of Santa Monica Basin, a broad anticline involves turbidite fill older than key reflector A, which is the deepest reflector that has been traced throughout the basin (Fig. 15A). The turbidite sequence between key reflectors A and J onlap the basinward flank of the anticline. The crest of the anticline is buried by about 100 m of the uppermost turbidites of the fan, but the crestal area of the anticline is cut by a fault that appears to extend to the modern sea floor (Fig. 15A). Continued movement on this fault has maintained a depression near the base of the slope, but structural relief has been minimized by deposition of undisturbed fill (Fig. 15B). There is no offset or folding of the upper 5 m of sediment (approximately midway between key reflector M and the sea floor) in the depression or on the lower Hueneme fan. Near the west end of the deep-tow boomer profile in Figure 15B, an offset of the Hueneme fan sequence that is not related to turbidite deposition is assumed to reflect flexure or faulting at the western limit of the flank of the anticline.

To the north of the profiles in Figure 15, a broad anticlinal crest reaches within 50 m of the sea floor (Fig. 16). In this case, key reflector A is clearly part of the sequence involved in the folding. By reflector B time, however, the Hueneme fan sequence onlaps and subsequently buries the fold. The deformation observed along the west edge of Santa Monica Basin in Figures 14 to 16 suggests a north-northwest trend, oblique to the trends of the mapped faults (Fig. 3) bounding the basin, but there is insufficient data to confirm this interpretation.

Southeast margin of Santa Monica Basin

South of the ODP Site 1015, the most easterly crossing of the basin margin shows basin plain deposits of the Hueneme fan onlapping a sequence of well-bedded sediment that forms the basin slope (Fig. 17). There is no structural disturbance of the turbidites in the basin-plain sequence at the base of the slope, but to the north, where the older basin paleoslope is buried by about 200 m of sediment, folding and tilting is observed in the basin fill generally below key reflector C (about 33 ka).

DISCUSSION

All of the profiles from the 1992 GSC/USGS survey that cross the margin of Santa Monica Basin show evidence for fold or fault (or both) disruption of the basin-fill turbidite deposits within the time encompassed by the key-reflector stratigraphy of Normark et al. (1998). This stratigraphy has been tentatively correlated with the ages of sediment cored at ODP Sites 893 and 1015 (Table 1; Shorebased Scientific Party, 1994; Shipboard Scientific Party, 1997). Figure 18 summarizes the timing of disruption of key reflectors as discussed above. It also shows the youngest key reflector affected, or where less precision is possible, the interval between key reflectors that shows the most recent evidence for disruption. The ages for key reflectors A and B assume that reflector A correlates with the top of isotopic stage 4; this assumption is reasonable given the correlations between the ODP Sites noted in Table 1.

The steep slopes on all sides of Santa Monica Basin (except for the southeast margin, which is formed by Redondo Knoll) suggest that these basin boundaries are among the most neotectonically active in the southern California borderland (Clarke et al., 1985; Greene and Kennedy, 1986; Vedder, 1987). The deeper-penetration sleeve-gun

seismic-reflection profiles show that deformation is taken up in anticlines at the northwestern end of the San Pedro Basin fault and along the fault systems bounding the western margin of Santa Monica Basin. Fold patterns are particularly complex in the northwestern margin of Santa Monica Basin, where oblique-slip motion on the northwest-trending faults passes into folding and thrusting associated with east-west faults parallel to the Transverse Ranges (Clarke et al., 1985; Greene and Kennedy, 1986; Vedder, 1987; Pinter et al., 1998; Figs. 3 and 18).

The main fault (or faults) along the southwestern margin of Santa Monica Basin has (have) not been imaged because of hyperbolic diffractions from the fault-line scarp that forms the steep basin slope, but secondary subparallel faults offset and tilt strata at depth (e.g., Fig. 5A). These faults are subvertical and show no systematic dip direction - a common feature of strike-slip faulting. Locally, near-surface sediment shows that tilting is similar to that at depth, but offsets of the youngest strata are not imaged. We assume that tilting of the turbidite sequence above reflector J means that recent (last 20 ka) offsets on the main fault are present at greater depth along the southwestern basin margin. The prominent unconformity created by this tilting (Fig. 13) suggests that motion is episodic, with a very large event at about 14 ka, i. e., that resulted in deformation of the sequence from reflectors J to L. An earlier similar event is visible from the onlap of basinal sediment on a strand of deformed sediment at about 28 ka (between key reflectors C and D; Figs. 14B and 19). The interval between episodes of major tilting in this part of Santa Monica Basin is about 14 ky, suggesting a risk of major displacement in the next few thousand years.

There is much evidence for recent fault offsets on the west-northwest trending secondary faults in the northwestern part of the basin; faults of this trend occupy a direction similar to Riedel shears with respect to the master basin-margin fault. We lack sufficient data to determine whether fold trends are oblique to these faults. Fault-dip directions are quite variable and some faults are marked by a fault-line sag (Fig. 15B), both characteristic of strike-slip faulting. The last demonstrable deformation observed in the deep-tow boomer profile of Figure 15B is estimated at about 9 ka (i.e., between key reflectors N and O).

The southern margin of Santa Monica Basin (Fig. 17) is defined by east-west trending bathymetric contours parallel to the faults at the northern margin of the basin. Some buried fault offsets are seen at this basin margin and, although we have insufficient data density to determine their trend, the bathymetry suggests that it is east-west (Fig. 19). The shallowest offsets are about 30 ka.

At the northern margin of the basin, major faulting with an east-west trend is indicated by the steep basin slope between Dume and Hueneme fans (Fig. 18). This main fault trace was crossed on several lines (those north of Lat. 33º 56' N; see Fig. 2), but its geometry is obscured by hyperbolic diffractions from the steep basin slope. Secondary faulting possibly associated with this zone is obscured by the irregular character of sediment progradation on Hueneme fan, where it is difficult to distinguish between surficial sediment failure, valley-wall erosion, and neotectonic fault offsets. A possible late Holocene fault break is seen in Figure 6C. Figure 6B suggests that a major splay of the main fault is marked by a steep slope resulting in hyperbolic diffractions; nevertheless, the profiles suggest that secondary faults might cut strata as young as 13 ka. We have no profiles farther west on

Hueneme fan along the strike of this fault trend, except possibly for the northern end of the only line that extends north of Lat. 34º west of Long. 119º 10' W (Figs. 2 and 3). The apparent lack of a strong morphological break on the upper Hueneme fan (as interpreted from NOAA chart NOS 1206N-15) may indicate that motion on the main fault is dispersed into a number of splays, of which Figure 6B shows only one, or that sedimentation here is rapid relative to the rate of vertical offset along the faults. The abundance of faults in the northwestern corner of the basin may be further evidence for dispersal of deformation. The limited evidence for recent fault disruption on the northern margin of the basin is probably a function of data distribution and the difficulty of imaging the main fault; it is not a convincing documentation for seismic inactivity.

The San Pedro Basin fault zone at the southeastern margin of the basin appears to be marked by a large number of fault splays rather than by a single main fault (Fig. 18). Toward the basin floor, anticlines, with or without faulting, become more abundant and some exhibit deformation of sediment younger than 5 ka. Surface breaks are visible on some profiles on the northeastern slope of the basin (Figs. 7 and 9). In some cases, near-surface fault offsets cannot be linked directly to deeper fault offsets (e.g. Fig. 9). The lack of a clear relation between near surface and deeper structures may be an acoustic artifact caused by hyperbolic diffractions, or may indicate that near-surface strata are deforming as a result of fault- or earthquake-induced bedding-plane sliding. This is an issue that requires further work. On the basin floor, the mound illustrated in Figure 11 appears to be a piercement structure resulting in deformation of the sea floor and of youthful strata.

Most surface breaks that suggest recent deformation (Figs. 6, 7, and 9) are on the northeastern margin of Santa Monica Basin. A widespread near-surface blocky debris flow just west of Dume Fan (Fig. 19) may have been seismically triggered and probably correlates with another debris-flow deposit on the floor of Santa Monica Basin just below reflector O (probably ca. 8 ka) (Fig. 13b in Piper et al., in press). The debris-flow deposit west of Dume fan, in particular, filled the easternmost of five valleys that have fed Hueneme fan during the last 50 ky. Filling of these valleys occurred at about the same time that the supply of sandy sediment was cut off as a result of rising sea level, estimated to be about 8.7 ka from the sea level curve of Fairbanks (1989). The lack of similar, more-deeply buried deposits suggests that this was an unusual event. Slumping on the northeastern basin margin took place a short distance below reflector L, at a horizon estimated to be about 14 ka (Figs 8, 12b, and 19). The only evidence for Holocene breaks on the western side of the basin is suggested in Figure 15A.

Our high-resolution seismic-reflection data contribute to determining recent seismicity in two ways. First, correlation is possible between these data and dated cores recovered at ODP Site 1015 throughout Santa Monica Basin, thus providing a chronological framework for interpreting seismic-reflection profiles (Shipboard Scientific Party, 1997). Second, in some cases, near-surface breaks can be identified in seismic-reflection profiles. In general, the large fault-line scarps created by master basin-bounding strike-slip faults generate hyperbolic diffractions that obscure evidence for recent breaks. Offsets along secondary faults with less topographic expression are recognizable, and the magnitudes and geometries of these displacements can be determined. In places, it is not clear whether the apparent lack of deformation in some seismic-reflection profiles results from diffractions, vertical exaggeration, and other acoustic artifacts, or whether some surface

and near-surface breaks result from soft-sediment detachment along bedding planes independent of faulting. Although some deformation, such as the growth of anticlines, appears quasi-continuous, in other places there is evidence of episodic fault motion. In both the northwest and southeast parts of the basin, the largest datable deformation event occurred about 14 ka, with a similarly large event in the northwest part of the basin at about 28 ka.

RECOMMENDATIONS FOR FURTHER STUDY

In 1998 the Western Coastal and Marine Geology Team will conduct the first of three major offshore surveys designed to evaluate the earthquake hazards posed by active faulting within the inner continental shelf and basin areas of the California continental borderland. Evaluation of the character of deformation and the determination of the recency and recurrence intervals for significant fault movement in the offshore area requires not only detailed surveys employing high-resolution reflection-seismic data, such as that available using the Huntec deep-tow boomer system, but also a direct method of dating sediment affected by the deformation. In addition, deeper-penetration data from high-resolution multichannel-profiling systems are needed to distinguish sedimentologic features, e.g., erosion-and-fill deposits or slide scars, from tectonic displacements. Correlation with ODP Site 1015 provides the best stratigraphic control in the Santa Monica Basin study area because the stratigraphy from this site can be extended to much of the basin and on to the adjacent slopes. The results of this review suggest that to take maximum advantage of the age data available from Site 1015, future surveys should:

1) provide a direct tie to Site 1015 with survey lines extending through the site and onto the slopes north and east of the drill site;

2) identify condensed sediment sections on the basin slopes that are directly correlative with the basin key-reflector stratigraphy dated by correlation with Site 1015; this will permit sediment coring using standard piston- or vibra-coring techniques that are generally limited to less than 10-m recovery;

3) obtain sufficient shallow and intermediate-to-deep seismic-reflection data in the very tectonically active northwestern corner of the basin to identify and map fault and fold trends that have not been recognized in previous structural analyses of the Santa Monica Basin area; and

4) map the complex pattern of faults that comprise the San Pedro Basin fault zone, which appears to have been active in the last 15 ka; this fault system is one of the closest offshore structures to the urban corridor of southern California and, as such, might pose a significant hazard to the area.

ACKNOWLEDGEMENTS

We thank the officers, crew, and technical staff of the Geological Survey of Canada who participated on CSS Parizeau cruise 91-062 for their assistance in gathering seismic data. Roy Sparkes was particularly helpful in preparation of trackplots and bathymetry of the Hueneme fan area. Reviews by Michael Marlow, Sam Clarke, and David Mosher resulted in improvements to the manuscript.

REFERENCES

Bohannon, R. G. and Geist, E., 1998, Upper crustal structure and Neogene tectonic development of the California continental borderland: Geol. Soc. Amer. Bull., v. 110, p. 779-800.

Christensen, C. J., Gorsline, D. S., Hammond, D. W., and Lund, S. P., 1994, Non-annual laminations and expansion of anoxic basin floor conditions in Santa Monica Basin, California Borderland, over the past four centuries. Mar. Geol., v. 116, p. 399-418.

Clarke, S. H., and Kennedy, M. P., 1997, Analysis of late Quaternary faulting in the Los Angeles Harbor area and hazard to the Vincent Thomas Bridge: California Dept. of Conservation, Division of Mines and Geology Open-File Report 97-10, 50p, 10 figures, 5 plates.

Clarke, S. H., Greene, H. G., and Kennedy, M. P., 1985, Identifying potentially active faults and unstable slopes offshore: *In* Ziony, J. I. (Ed), Evaluating earthquake hazards in the Los Angeles region: an earth-science perspective: U.S. Geological Survey Professional Paper 1360, p. 347-496.

Crouch, J. K. and Suppe, J., 1993, Late Cenozoic tectonic evolution of the Los Angeles Basin and inner California Borderland: a model for core complex-like crustal extension: Geol. Soc. Amer. Bull., v. 105, 1415-1434.

Dolan, J. F., Sieh, K., Rockwell, T. K., Guptill, P., and Miller, G., 1997, Active tectonics, paleoseismology, and seismic hazards of the Hollywood fault, northern Los Angeles basin, California: Geol. Soc. Amer. Bull., v. 109, p. 1595-1616.

Edwards, B. D., Field, M. E., and Kenyon, N. H., 1996, Morphology of small submarine fans, inner California Continental Borderland: *In* Gardner, J.V., Field, M. E., and Twitchell, D. G. (Eds), Geology of the United States' Seafloor: The View from GLORIA, Cambridge Univ. Press (Cambridge), p. 235-249.

Fairbanks, R. G., 1989, A 17,000-year glacioeustatic sea level record: influence of glacial melting rates of the Younger Dryas event and deep-ocean circulation. Nature, v. 342, p. 637-642.

Gorsline, D. S., 1996, Depositional events in Santa Monica Basin, California Borderland, over the past five centuries: Sediment. Geol., v. 104, p. 73-88.

Gorsline, D. S. and Emery, K. O., 1959, Turbidity-current deposits in San Pedro and Santa Monica basins off southern California: Geol. Soc. Amer. Bull., v. 70, p. 279-290.

Greene, H. G. and Kennedy, M. P., eds, 1986, Geology of the mid-southern California continental margin --- Area 2 of 7: California continental margin geologic map series: Sacremento, CA (California Division of Mines and Geology), scale 1:250,000.

Kennett, J. P., and Venz, K., 1995, Late Quaternary climatically related planktonic foraminiferal assemblage changes: Hole 893A, Santa Barbara Basin, California. *In* Kennett, J. P., Baldauf, J. G., and Lyle, M. (Eds), *Proc. ODP, Sci. Results*, 146 (Pt. 2): College Station, TX (Ocean Drilling Program), p. 281-293.

Klitgord, K.D., and Brocher, T., 1996, Oblique-slip deformation in the San Pedro Basin offshore Southern California: EOS, Trans. Amer. Geophys. Union, v. 77, p. F737.

Legg, M. R., 1991, Developments in understanding the tectonic evolution of the Califronia Continental Borderland: SEPM Society for Sedimentary Geology Special Publication 46, p. 291-312.

Mutti, E., and Normark, W. R., 1987, Comparing examples of modern and ancient turbidite systems: Problems and concepts: *In* Leggett, J. K., and Zuffa, G. G. (Eds), Marine Clastic Sedimentology, Graham and Trotman (London), p. 1-38.

Nardin, T. R., 1981, Seismic stratigraphy of Santa Monica and San Pedro Basins, California continental borderland: late Neogene history of sedimentation and tectonics: thesis, University of So. California, Los Angeles.

Nardin, T. R., 1983, Late Quaternary depositional systems and sea level change --- Santa Monica and San Pedro Basins, California Continental Borderland: Amer. Assoc. Petroleum Geol. Bull., v. 67, p. 1104-1124.

Normark, W. R., Piper, D. J. W., and Hiscott, R. N., 1998, Sea level controls on the textural characteristics and depositional architecture of the Hueneme and associated submarine fan systems, Santa Monica Basin, California: Sedimentology, v. 45, p. 53-70.

Pinter, N., Lueddecke, S. B., Keller, E. A., and Simmons, K. R., 1998, Late Quaternary slip on the Santa Cruz Island fault, California: Geol. Soc. Amer. Bull., v. 110, p. 711-722.

Piper, W. R., Hiscott, R. N., and Normark, W. R., in press, Outcrop-scale acoustic facies analysis and the 0 - 15 ka development of Hueneme and Dume fans, California Continental Borderland: Sedimentology, v. 45,

Piper, D. J. W., W. R. Normark, and R. N. Hiscott, 1995, Chp. 28: Holocene sand body geometry, Hueneme Fan, California Borderland, in An Atlas of Deep-Water Environments: Architectural Style in Turbidite Systems, ed.by Pickering, K. T., Hiscott, R. N., Kenyon, N., Ricci Lucchi, R., Smith, R.; Chapman and Hall, London, p. 203-206.

Reynolds, S., 1987, A recent trubidity current event, Hueneme fan, California: reconstruction of flow properties. Sedimentology, v. 34, p. 129-137.

Schwalbach, J. R. and Gorsline, D. S., 1985, Holocene sediment budgets for the basins of the California continental borderland: Jour. Sed. Petrology, v. 55, p. 829-842.

Shipboard Scientific Party, 1997, Site 1015, *In* Lyle, M., Koizumi, I., Richter, C., et al., *Proc. ODP, Init. Repts.*, 167: College Station, TX (Ocean Drilling Program), p. 223-237.

Shorebased Scientific Party, 1994, Site 893, *In* Kennett, J. P., Baldauf, J., et al., *Proc. ODP, Init. Repts.*, 146, pt. 2: College Station, TX (Ocean Drilling Program), p. 15-50.

Vedder, J. G., 1987, Regional geology and petroleum potential of the Southern California Borderland, In Scholl, D. W., Grantz, A., and Vedder, J. G., eds., Geology and Resource Potential of the Continental Margin of Western North America and Adjacent Ocean Basins --- Beuafort Sea to Baja California, Circum-Pacific Council for Energy and Mineral Resources Earth Science Series, v. 6 (Houston, TX), p. 403-447.

Wallace, R. E., ed., 1990, The San Andreas Fault System, California: U.S. Geological Survey Professional Paper 1515, 283 pp.

Ziony, J. I., and Yerkes, R. F., 1985, Evaluating earthquake and surface-faulting potential: *In* Ziony, J. I. (Ed), Evaluating earthquake hazards in the Los Angeles region: an earth-science perspective: U.S. Geological Survey Professional Paper 1360, p. 43-91.

Table 1. Tentative age of key reflectors[1]

Reflector [2]	Depth in two-way travel time (ms)	Core depth at ODP Site 1015 (m)	Tentative age (ka)	Basis of age
O	4	4	5-8	Extrapolation of box core sedimentation rates
N	14	11	10-11	Sedimentation rates, sedimentological response to sea-level standstill
M	21	16	12	Interpolated from foram pick of 15 ka at 26 meters below sea floor (mbsf)
L	25	19	13.5	Interpolated from foram pick of 15 ka at 26 mbsf
J	45	36	16	Interpolated from foram pick of 18 ka at 70 mbsf
F	87	70	18	Foram pick (see text)
D	120	96	23	Interpolated from foram stratigraphy at 70 and 144 mbsf
C	180	144	33	Preliminary foram stratigraphy, < 65 ka on nannofossils
B		3	~50	Interpolated based on sedimentation rates and the assumptions below for key reflector A
A		3	~70	Extrapolation based on sedimentation rates and on evidence for a sea-level low-stand interval interpreted to be isotopic stage 4 (~60 to 80 ka) in the seismic stratigraphy of Dume Fan; note that this interpretation is revised from Normark et al. (1998).

(1) Age picks are based on the preliminary biostratigraphy from ODP Site 1015 presented in Shipboard Scientific Party (1997) reinterpreted through correlation with ODP Site 893 (Shorebased Scientific Party, 1994) as discussed on p. 8 in this report; these age assignments are revised from those presented in Normark et al. (1998) for the key-reflector stratigraphy.

(2) Age estimates are for reflectors as defined on the lower fan and basin plain. The reflector correlated as J on the upper fan may be a little older.

(3) Maximum depth cored at Site 1015 is 149.5 mbsf (Shipboard Scientific Party, 1997).

Table 2. Key features observed in the seismic-reflection profiles that are used for the compilation of the timing of deformation schematically shown in Figure 18.

Figure #	Key features for determining timing of deformation shown in Figure 18
5C	Post reflector-N strata tilted at basin margin.
6B	Shallowest fault trace extends from the interval below reflector C to about reflector M and might reach sea floor.
7	Most mid-slope faults (denoted San Pedro Basin fault traces) appear to extend to sea floor (see also Fig. 9); faults and folds at base of slope that are buried by basin-plain turbidites were active at least until reflector C and uplift may have continued affecting reflector J.
8	Fault (queried) shows offset of strata as shallow as the interval between reflectors J -L; buried slide deposit is overlain by reflector L.
10	The shallowest of two mid-slope faults, identified as SPBF, extends to the sea floor; an adjacent fault strand (denoted SPBF?) appears draped by recent sedimentation.
11	The piercement structure is bounded by faults that appear to extend to the sea floor.
12A	Growth fold is active at least until reflector L and possibly affects even younger strata (the zone of upbowing is noted in the figure)
12B	Buried slide deposit is overlain by reflector L.
13	Sediment on floor of graben is tilted and unconformably overlies more steeply dipping strata from the interval between reflectors J to L. Strata of Hueneme fan post reflector N have been affected by gentle tilting and/or slumping; most recent sediment may be truncated by faulting or slumping.
14A	Faulting affects pre-reflector J strata and folding involves strata in the interval between reflectors J and M.
14B	Faulting extends into the interval between reflectors B and C and tilting of strata in the interval between reflectors C and D is similar to a younger event observed in Figure 13. Folding involves strata in the interval between J and M and possibly as young as reflector M .
15A,B	Faulting and deformation involves post-reflector-M strata and probably extends to the present sea floor except for a thin, recent sediment fill in a depression along the fault trace (Fig. 15B).
16	Folding involves strata as young as the interval between reflectors J and M.

FIGURE CAPTIONS

Figure 1. Major geographic and physiographic features of the California continental borderland and adjacent coastal area; modified from Vedder (1987). The 200 m and 750 m contours are used to outline the continental shelf and the major ridge and basin areas of the borderland. Box indicates area of study shown in Figures 2 and 3. Solid diamonds shows Site 893 of Ocean Drilling Program Leg 146 in Santa Barbara Basin (Shorebased Scientific Party, 1994) and Site 1015 in Santa Monica Basin (Shipboard Scientific Party, 1997). A star indicates the epicenter of the onshore 1994 Northridge earthquake.

Figure 2. Trackline map for cruise 91-062, a cooperative survey conducted by the Geological Survey of Canada and the U. S. Geological Survey in early 1992. Solid diamond indicates Site 1015 of Ocean Drilling Program Leg 167 (Shipboard Scientific Party, 1997). Box indicates the area of Figure 4 inset map and survey lines 13, 36, and 57 are in shown as bold lines. Areas of Hueneme and Dume fans and the canyons that supply sediment to the fans are indicated. Bathymetry based on NOAA chart NOS 1206N-15.

Figure 3. Fault pattern in Santa Monica Basin (from K. D. Klitgord, written communication, 1997). The fault pattern is in part schematic and many of the faults depicted appear to be complex zones with multiple strands commonly associated with minor folding locally. The fault pattern is based on interpretations by Clarke et al. (1985), Greene and Kennedy (1986), Vedder (1987), Wallace (1990), and Legg (1991). This report shows that many of the faults depicted appear to be fault zones with multiple strands or with associated structures; because of the limited data for this study, it is not possible to redraw the fault pattern in more detail at this time. Areas of Hueneme and Dume fans are indicated. Locations of seismic-reflection profiles in Figures 5 to 17 are shown.

Figure 4: Line drawings of seismic-reflection profiles from Hueneme and Dume fans in Santa Monica Basin illustrating the stratigraphic expression of some of the key reflectors (identified by block letters) that can be mapped in many parts of the basin. The correlations on Line 36, which is a strike profile on the upper Hueneme fan, cannot be carried across the profile because of the erosion and fill associated with a series of leveed fan valleys; the key reflectors can be brought into this profile on dip lines, however, because of the much greater reflector continuity on the lower fan and basin plain areas.

Figure 5. Comparison of vertical resolution and depth of acoustic penetration for the three seismic-reflection systems used for the Santa Monica Basin study; see methods in text for details. Key reflectors indicated by block letters. A) low-frequency record collected with 30-m SE streamer shows possible fault contacts and folding of deeper basin-fill sediment at the basin margin along a zone of deformation; the dominantly turbidite fill generally onlaps the basin margin in the upper 100 m with no clear structural disruption except a gentle upwarp of sediment from just below key reflector F. Inset map shows the location of the profiles in this figure with respect to the survey tracklines and faults shown in Figures 2 and 3. B) The record obtained with the NSRF streamer shows a distinct unconformity at about 40 m depth (key reflector J) and that the basin fill is upwarped at the margin; in addition, this record shows variable

acoustic character within the turbidite fill that can be used to define depositional elements and/or acoustic facies. C) The corresponding deep-tow boomer profile at the base of the slope shows evidence for offset and tilting within the upper 20 m of the basin turbidites suggesting relatively recent movement on the basin-bounding fault.

Figure 6. A and B: Seismic-reflection profiles (30-m SE) showing possible disruption along basin-margin faults at depth. In Figure 6A, the faults closest to the southern end of the profile appear to indicate disruption in the general area of the basin floor where two faults are shown in the generalized compilation of basin structures in Figures 3. Figure 6B shows multiple strands(?) in the area of the fault shown near the base of the northern slope margin of Santa Monica Basin. Inset map shows the location of the profiles in this figure with respect to the survey tracklines and faults shown in Figures 2 and 3. Key reflectors indicated by block letters. In seismic-reflection profiles across the northern margin of the basin, the effects of faulting are difficult to distinguish within the turbidite fill, which commonly shows extensive mass-wasting as well as erosion and fill features within a series of stacked submarine-fan channels (Normark et al., 1998; Piper et al., in press). C) Deep-tow boomer profile at the base of the slope along the north side of the basin (see text).

Figure 7. Seismic-reflection profile (30-m SE) that crosses several possible strands of the San Pedro Basin fault trend and two short fault segments that trend northwest-southeast along the eastern margin of Santa Monica Basin. This seismic-reflection profile suggests that faulting is broadly distributed with respect to both of the structural trends noted above; for both trends, there are more fault strands than indicated in existing compilations. Inset map shows the location of the profiles in Figures 7 to 9 with respect to the survey tracklines and faults shown in Figures 2 and 3. The location of the higher resolution deep-tow boomer profiles from the base of the slope (Fig. 8) and the San Pedro Basin fault (Fig. 9) are shown with thicker line weight. C/C indicates course change. Key reflectors indicated by block letters.

Figure 8. Deep-tow boomer profile at the base of the slope along the northeastern side of Santa Monica Basin showing slide deposit and possible offset of deeper horizons below reflector L (see text). Key reflectors indicated by block letters. Location shown in Figures 3 and 7.

Figure 9. Deep-tow boomer profile showing multiple strands of faults on strike with the suggested trace of the San Pedro Basin fault (see location in Figs. 3 and 7). Key reflectors indicated by block letters. Offset of the sea floor on two of the strands suggests recent activity perhaps related to slump failure.

Figure 10. Seismic-reflection profile (30-m SE) southeast of the tracklines of Figures 7 to 9 along the northeastern margin of Santa Monica Basin showing possible displacements related to faults the San Pedro Basin Fault trend. Inset map shows the location of the profiles in Figures 10 and 11 with respect to the survey tracklines and faults shown in Figures 2 and 3. SPBF indicates San Pedro Basin fault, queried where uncertain. 'Crossing 6' is discussed in the text.

Figure 11. Deep-tow boomer profile across a diapir-like piercement structure that shows basin sediment thinning by 30% against faulted (?) flanks of this feature. Location

given in Figures 3 and 10. This piercement structure lies between the fault traces compiled from previous work (Fig. 3).

Figure 12. Deep-tow boomer profiles along the southeastern margin of Santa Monica Basin on the northwestern side of Redondo Knoll (Fig. 1). Inset map shows the location of the profiles in this figure with respect to the survey tracklines and faults shown in Figures 2 and 3. A: Uplift of turbidite fill in the southern half of this profile is more pronounced below reflector L, which is the only key reflector that can be identified in this part of the basin, but affects sediment to within two meters of the sea floor in the zone of upbowing. B: A buried slide along the base of the slope below reflector L that may be contemporaneous with a similar deposit in Figure 8.

Figure 13. Deep-tow boomer profile showing upbowing of deeper sections of Hueneme fan with a depositional unconformity in a depression at the base of the slope. Inset map shows the location of the profiles in this figure with respect to the survey tracklines and faults shown in Figures 2 and 3. Key reflectors indicated by block letters.

Figure 14. Seismic-reflection profiles (NSRF) near the western corner of Santa Monica Basin showing faulted flanks of buried folds. Inset map shows the location of the profiles in this figure with respect to the survey tracklines and faults shown in Figures 2 and 3. Key reflectors indicated by block letters. Both profiles in Figure 14 show that faulting within the older basin sediment is more distributed than is suggested by the compilation of Figure 3. A: Deformation has clearly affected sediment of reflector J and below but the youngest turbidites of Hueneme fan have effectively smoothed the sea floor. The profile is from a broad turn (c/c = changing course) that leads to the straight course of Figure 14B. B: This profile is continuous with the southern end of part A and shows the turbidites of the fan downlapping on the anticline flank at, and just shallower than, reflector J. Both 14A and 14B show the basin fill is upwarped near the basin margin.

Figure 15. A: Seismic-reflection profile (30-m SE) showing folding of older basin turbidite fill along a fault in the western corner of Santa Monica Basin. the faults identified in this transect lie between the structures shown in the compilation of Figure 3. Inset map shows the location of the profiles in this figure with respect to the survey tracklines and faults shown in Figures 2 and 3. Key reflectors indicated by block letters. Location of Figure 15B is shown as thicker line weight. Basin-fill sediment from below reflector B to the sea floor onlap and bury the anticlinal structure; faulting of the fold cuts to the present sea floor and is marked by a depression at the base of the slope. B: Deep-tow boomer profile from the western end of Figure 15A showing that sediment younger than reflector M, but not the sea floor, is affected by displacement along the fault. The depression is under the scale bars.

Figure 16. Seismic-reflection profiles (30-m SE) showing folding and faulting of older basin turbidite fill near the western corner of Santa Monica Basin. The faults observed in the profile suggest a broad zone of disruption rather than just the two fault traces depicted in Figure 3. Inset map shows the location of the profile with respect to the survey tracklines and faults shown in Figures 2 and 3. Key reflectors indicated by block letters. Anticlinal structure in center of this profile formed before reflector B,

which onlaps the northeast flank; to the southwest, the sea floor is offset along a fault near the base of the slope.

Figure 17. Seismic-reflection profile (30-m SE) showing that faults in the southern corner of Santa Monica Basin are buried by Hueneme fan sediment above reflector C; the sediment onlapping on this relatively low gradient basin slope is not affected by recent faulting. Inset map shows the location of the profile with respect to the survey tracklines and faults shown in Figures 2 and 3. Key reflectors indicated by block letters.

Figure 18. Summary of observed timing of deformation in Santa Monica Basin based on youngest key reflector affected. Table 2 reviews the key features observed in the seismic-reflection profiles that are used for the compilation of timing of deformation. The center of the solid ellipses approximates the point along the track where the deformation was observed, the long axis indicates suspected trend of faults or folds, and the associated letter indicates the youngest key reflector affected. A range of stratigraphic markers, e.g., J-M indicates movement occurred after deposition of J but before key reflector M was deposited (between 12 and 16 kya). The annotation SF? indicates that deformation might involve the sea floor, but there is no stratigraphic control, e.g. where the fault lies along the axis of a canyon or gully feature. In the western corner of the basin, which appears to be the most common site for Holocene activity, deformation is observed on apparent north-south fault/fold trends that have not been previously identified.

Figure 19. Schematic illustration of the timing and location of structural features and depositional events in Santa Monica Basin thought to reflect movement on the fault systems bounding the basin. Steep basin slopes on the north and southwest margins of the basin are thought to reflect major fault zones (see text references and Figure 3). These steep slopes are poorly imaged by all of the seismic-reflection systems, however, and the deformation observed is typically in sediment fill adjacent to these slopes. The youngest offsets or folding of strata shown might, in some cases, aid in determination of recurrence intervals of the deformation events if the extent of the structures can be adequately mapped with additional data. For example, the southwestern margin of Santa Monica Basin shows several episodes of tilting of basin-fill turbidites at about 14 ka and 28 ka, e.g., compare Figures 13 and 14B (with Table 2) and see discussion in text. The indication of surface break means only that the faults denoted appear to affect the youngest sediment, e.g., Figure 9. In other profiles, however, effect of their high vertical exaggeration might cause flexures to appear as breaks so not all possible 'surface breaks' have been plotted.

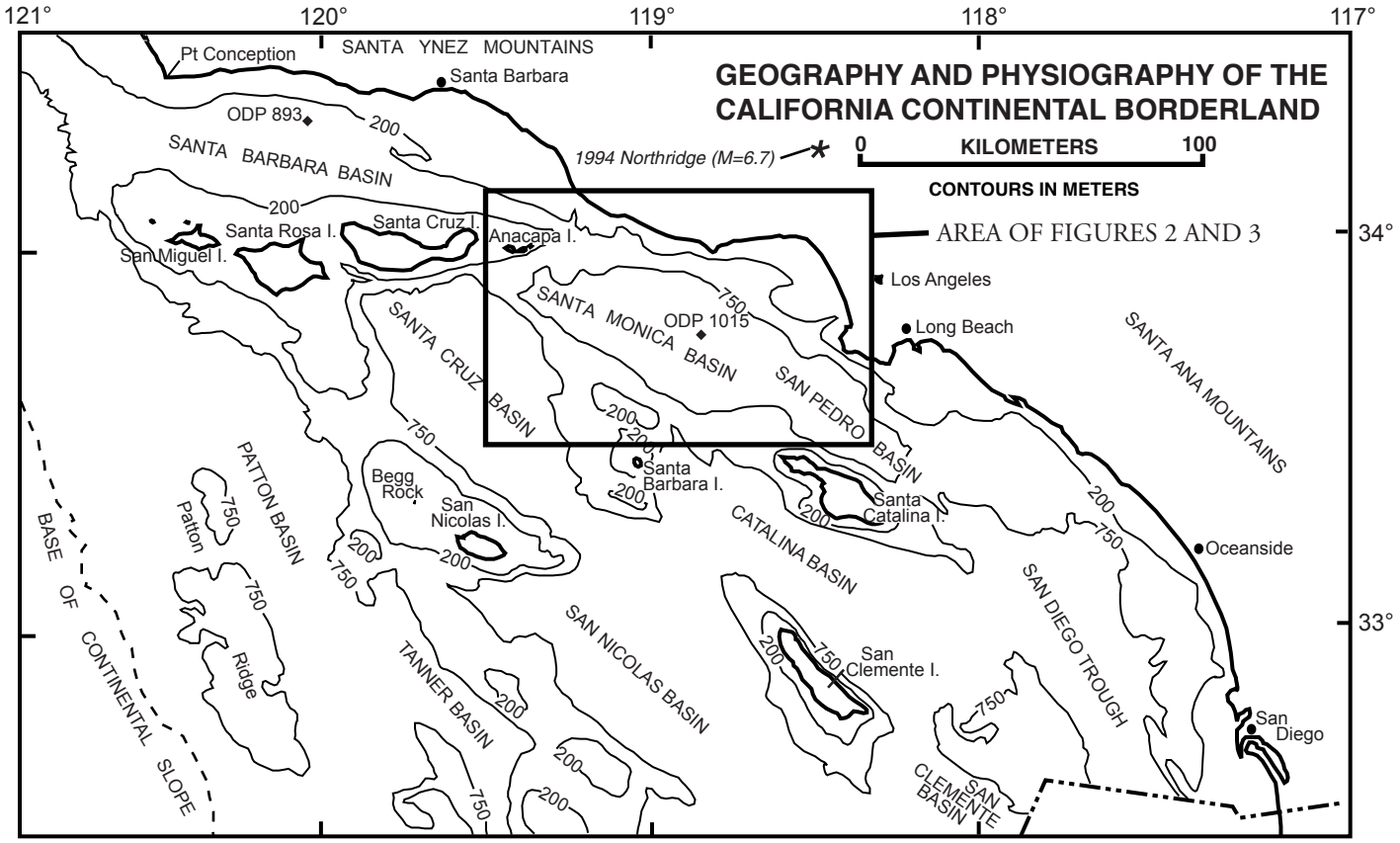
GEOGRAPHY AND PHYSIOGRAPHY OF THE CALIFORNIA CONTINENTAL BORDERLAND
121°
120°
119°
118°
117°
34°
33°
Pt Conception
SANTA YNEZ MOUNTAINS
Santa Barbara
ODP 893
SANTA BARBARA BASIN
1994 Northridge (M=6.7)
0 KILOMETERS 100
CONTOURS IN METERS
AREA OF FIGURES 2 AND 3
Santa Rosa I.
Santa Cruz I.
Anacapa I.
San Miguel I.
Los Angeles
Long Beach
SANTA MONICA BASIN
ODP 1015
SANTA CRUZ BASIN
SAN PEDRO BASIN
SANTA ANA MOUNTAINS
Santa Barbara I.
Santa Catalina I.
Oceanside
Begg Rock
San Nicolas I.
PATTON BASIN
Patton Ridge
BASE OF CONTINENTAL SLOPE
CATALINA BASIN
SAN DIEGO TROUGH
SAN NICOLAS BASIN
TANNER BASIN
San Clemente I.
San Diego
SAN CLEMENTE BASIN
200
750

Figure 1

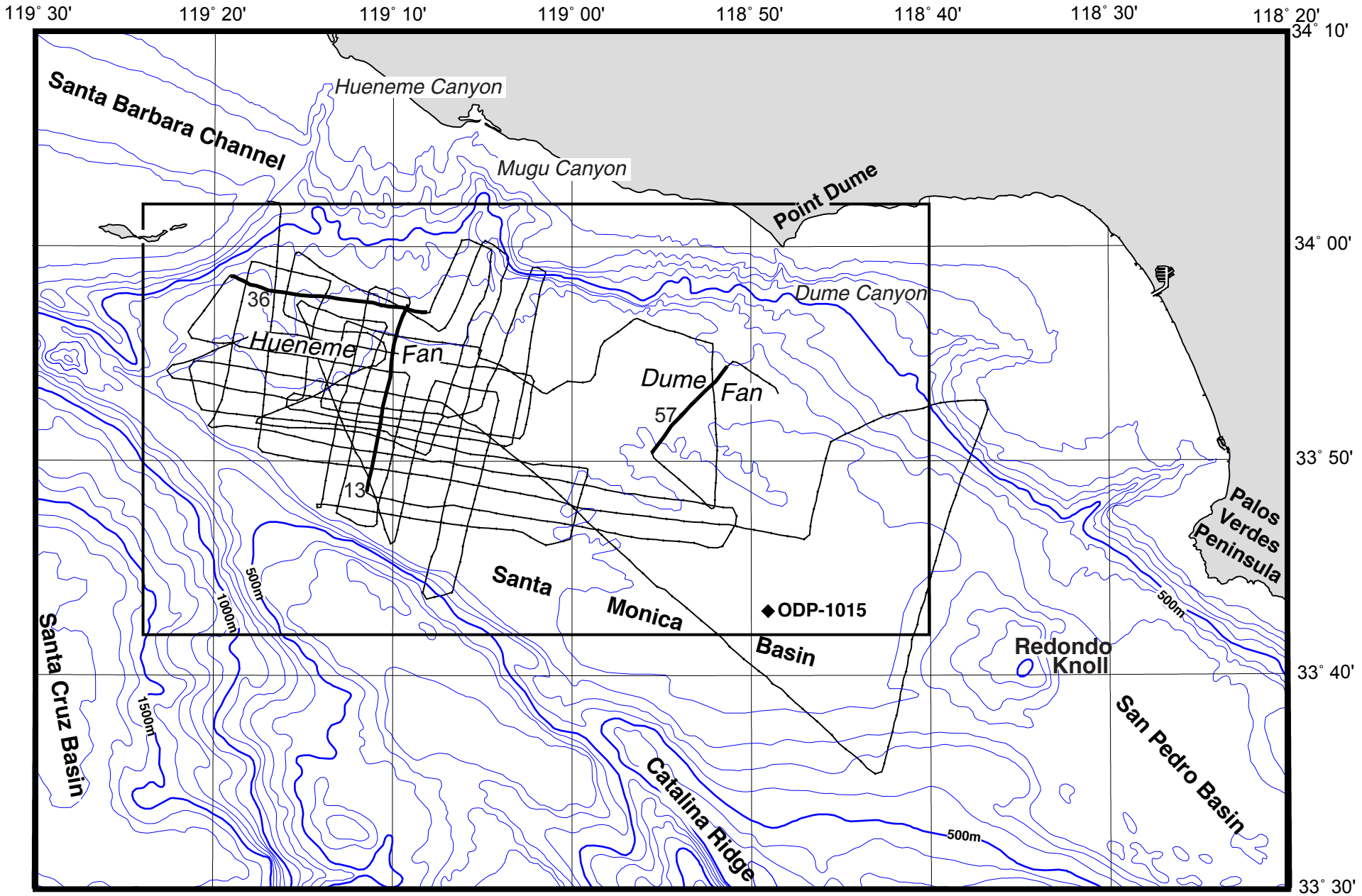
119° 30'
119° 20'
119° 10'
119° 00'
118° 50'
118° 40'
118° 30'
118° 20'
34° 10'
34° 00'
33° 50'
33° 40'
33° 30'
Santa Barbara Channel
Hueneme Canyon
Mugu Canyon
Point Dume
Dume Canyon
36
Hueneme Fan
Dume Fan
57
13
Santa Monica Basin
ODP-1015
Palos Verdes Peninsula
Redondo Knoll
San Pedro Basin
Santa Cruz Basin
Catalina Ridge
500m
1000m
1500m

Figure 2

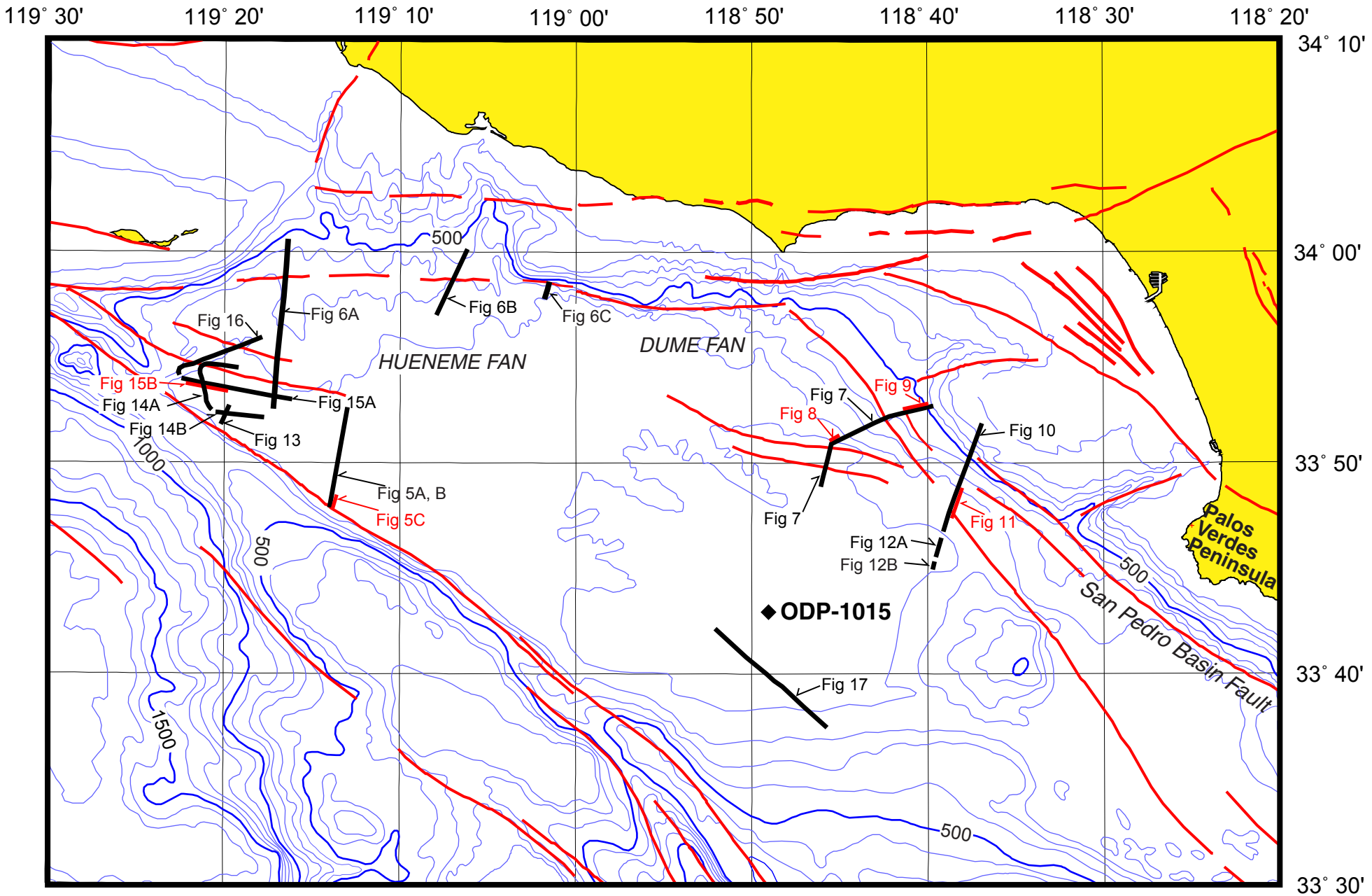
119° 30'
119° 20'
119° 10'
119° 00'
118° 50'
118° 40'
118° 30'
118° 20'
34° 10'
34° 00'
33° 50'
33° 40'
33° 30'
Fig 16
Fig 6A
500
Fig 6B
Fig 6C
HUENEME FAN
DUME FAN
Fig 15B
Fig 14A
Fig 14B
Fig 13
Fig 15A
1000
Fig 5A, B
Fig 5C
500
Fig 7
Fig 9
Fig 8
Fig 10
Fig 7
Fig 11
Fig 12A
Fig 12B
Palos Verdes Peninsula
500
San Pedro Basin Fault
ODP-1015
Fig 17
1500
500

Figure 3

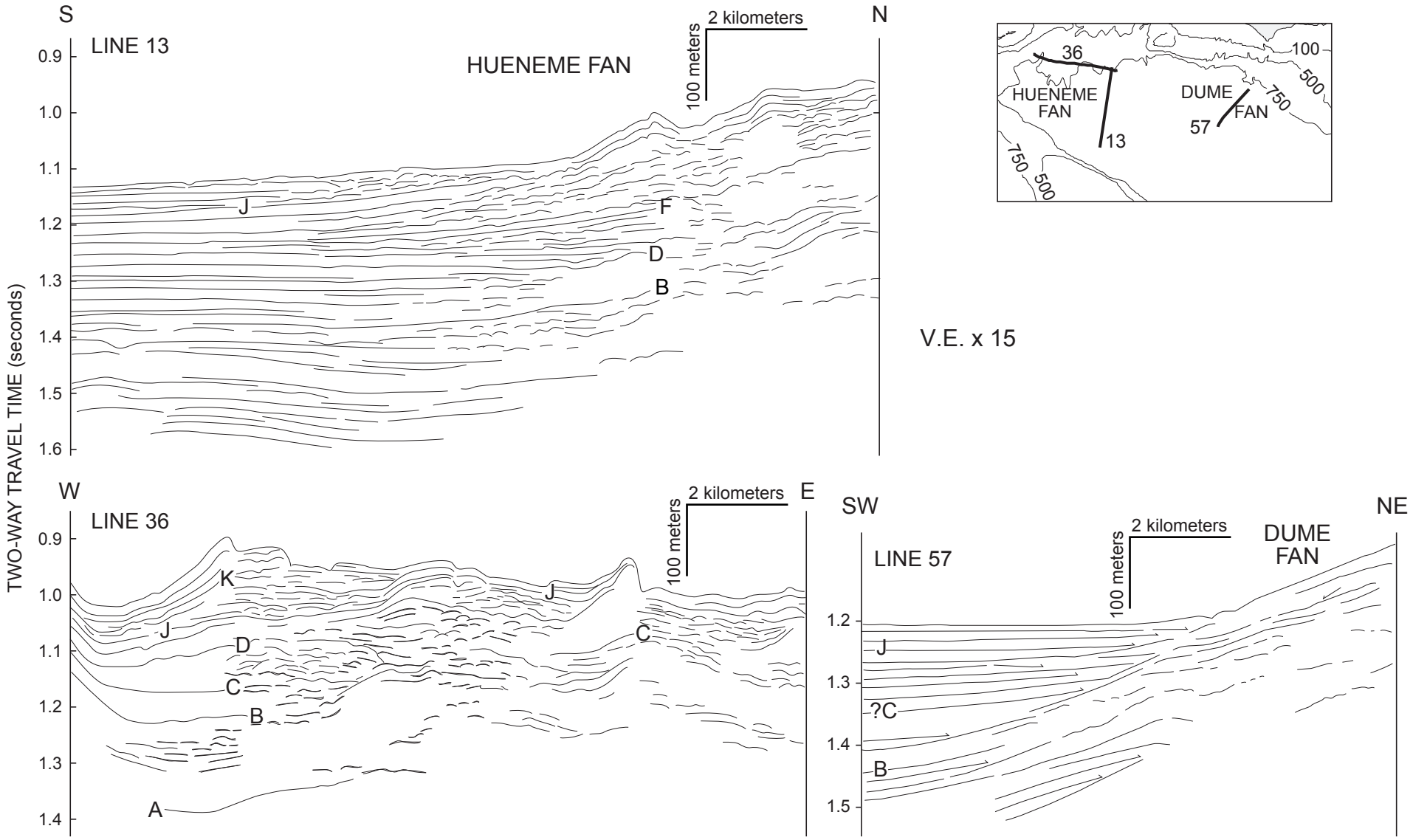
S
LINE 13
HUENEME FAN
2 kilometers
100 meters
N
0.9
1.0
1.1
1.2
1.3
1.4
1.5
1.6
J
F
D
B
TWO-WAY TRAVEL TIME (seconds)
36
100
500
750
HUENEME FAN
DUME FAN
57
13
V.E. x 15
W
LINE 36
2 kilometers
100 meters
E
K
J
D
C
B
A
SW
LINE 57
2 kilometers
100 meters
DUME FAN
NE
?C

Figure 4

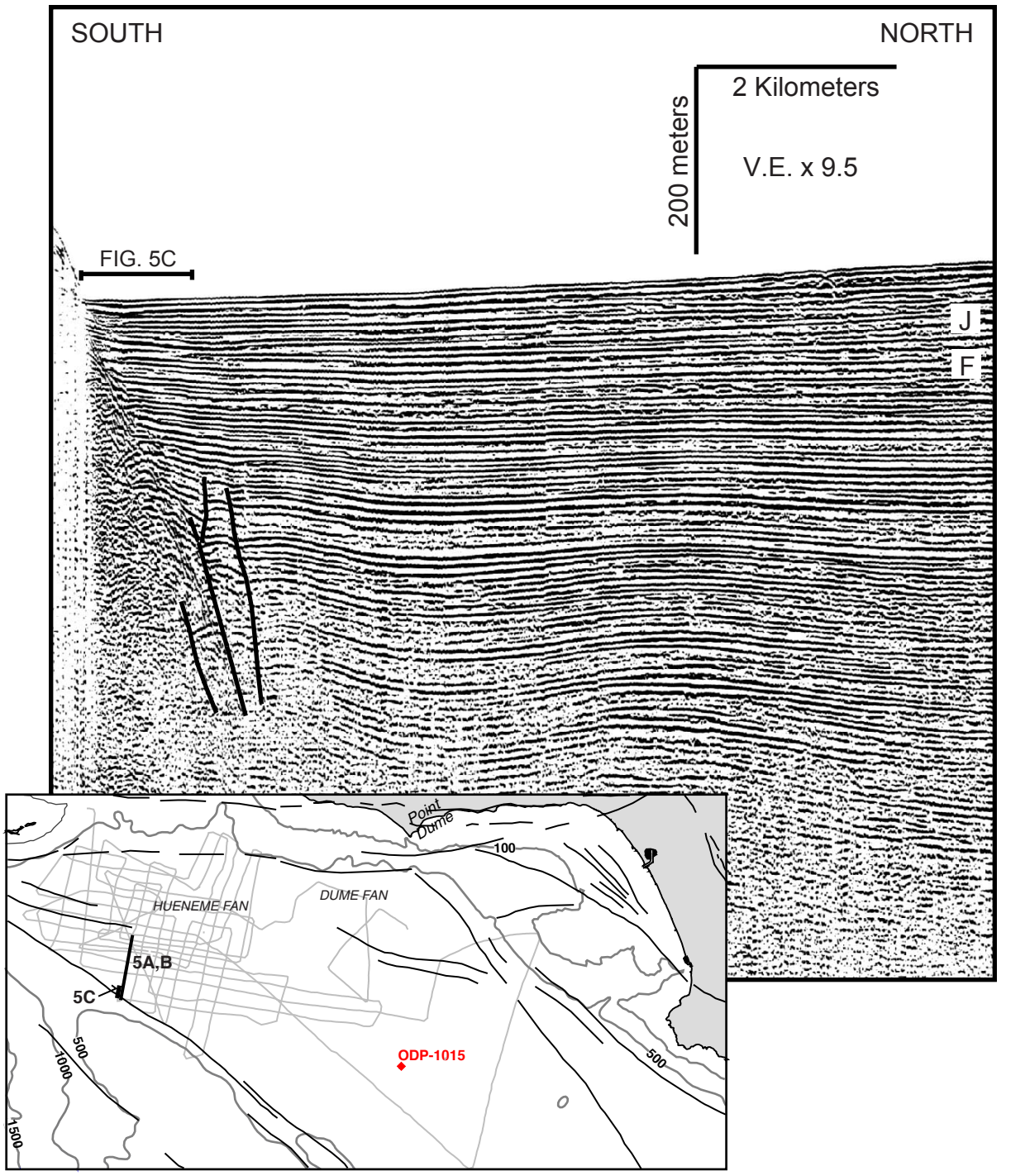
SOUTH
NORTH
2 Kilometers
200 meters
V.E. x 9.5
FIG. 5C
J
F
Point Dume
100
HUENEME FAN
DUME FAN
5A,B
5C
500
1000
1500
ODP-1015
500

Figure 5A

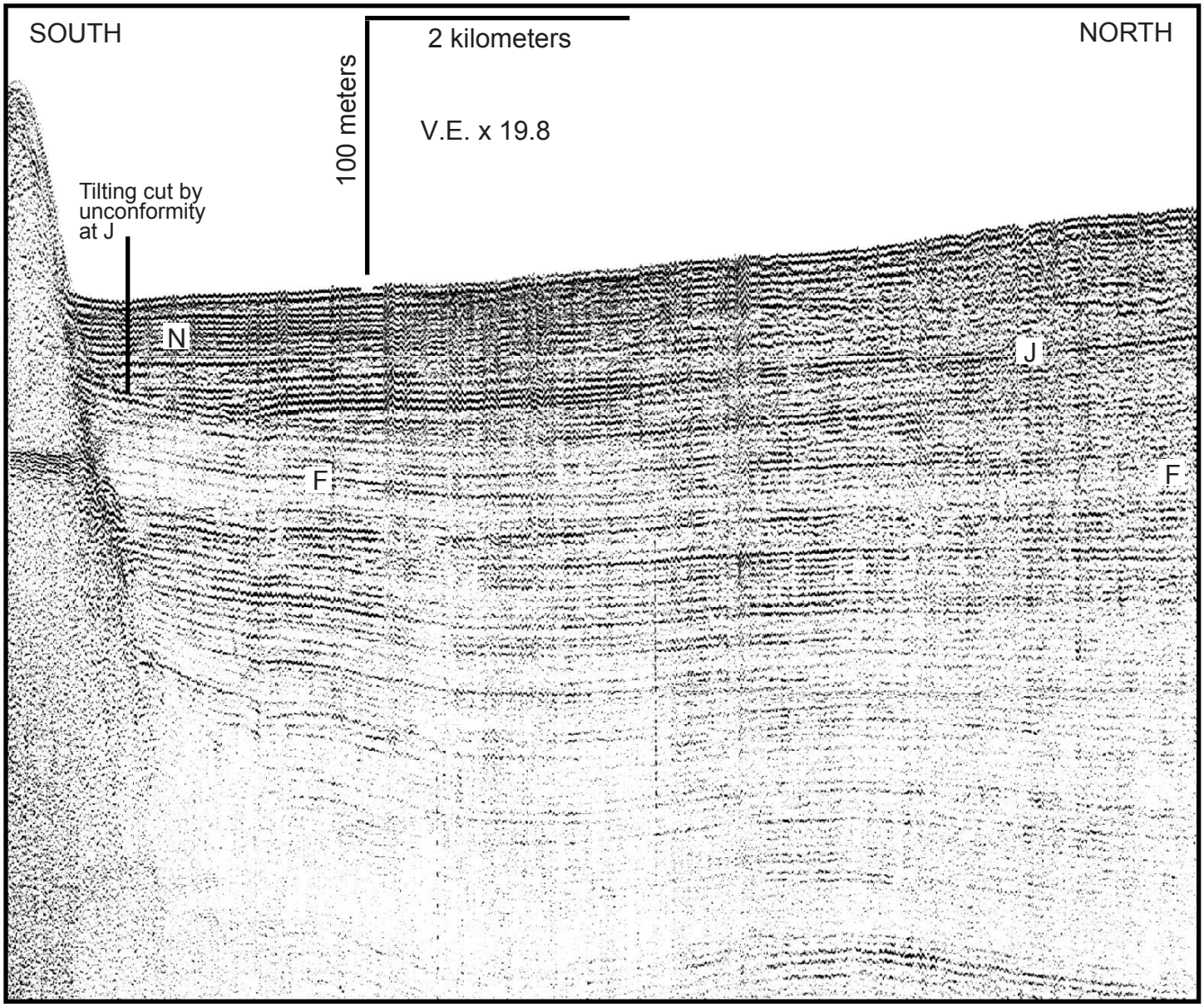
SOUTH
2 kilometers
NORTH
100 meters
V.E. x 19.8
Tilting cut by
unconformity
at J
N
J
F
F

Figure 5B

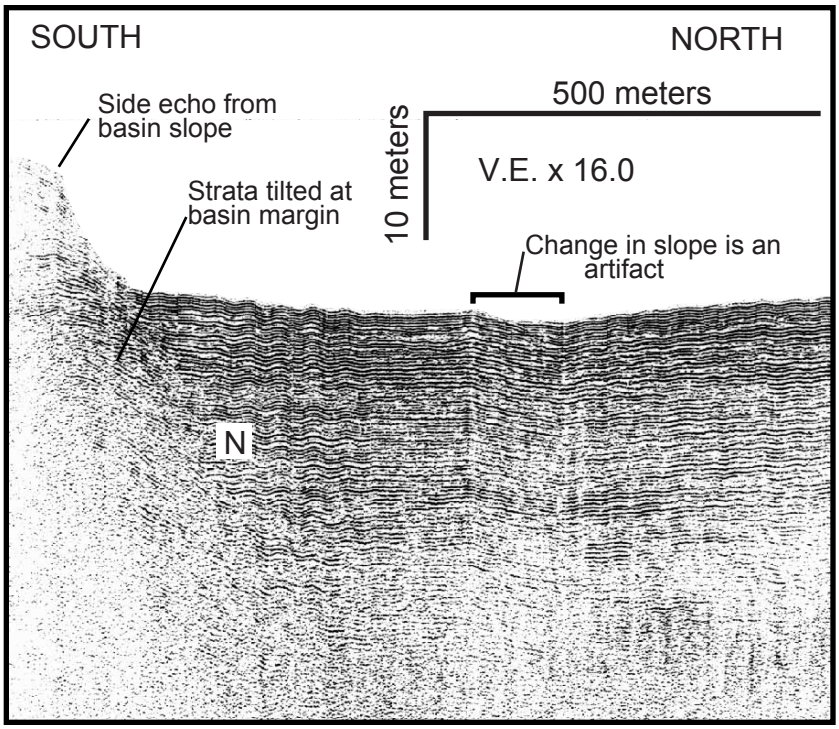
SOUTH
NORTH
Side echo from basin slope
500 meters
10 meters
V.E. x 16.0
Strata tilted at basin margin
Change in slope is an artifact
N

Figure 5C

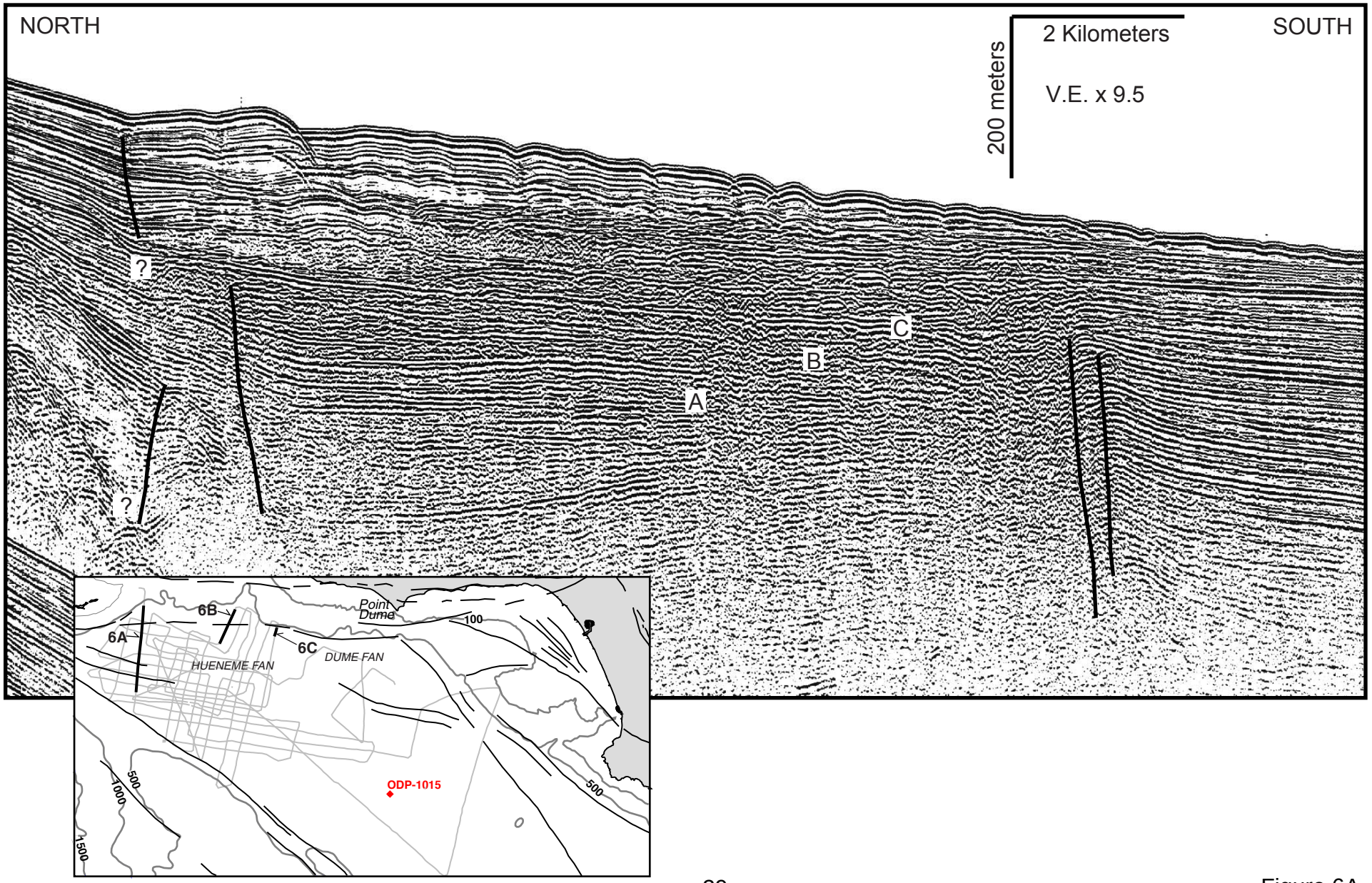
NORTH
SOUTH
2 Kilometers
V.E. x 9.5
200 meters
?
?
A
B
C
6A
6B
6C
HUENEME FAN
DUME FAN
Point Dume
100
500
1000
1500
500
ODP-1015

Figure 6A

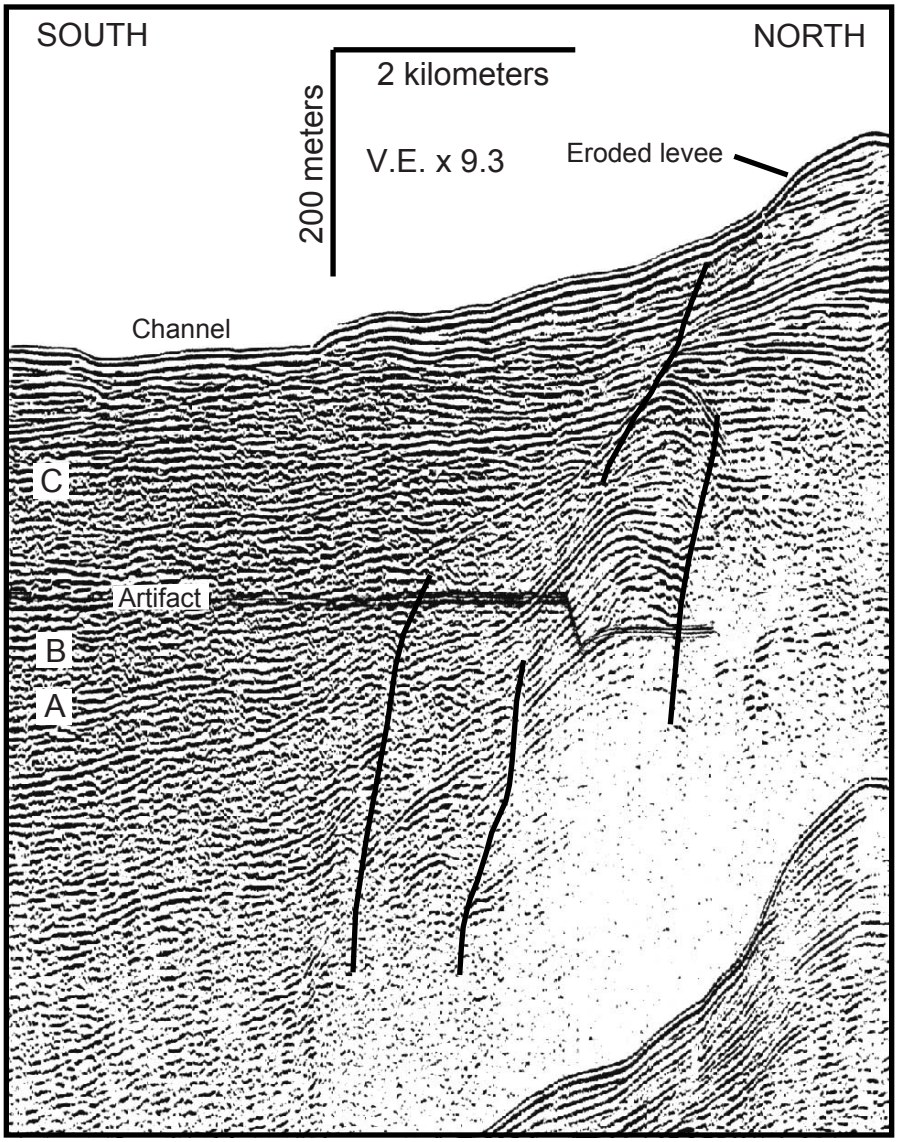
SOUTH
NORTH
2 kilometers
200 meters
V.E. x 9.3
Eroded levee
Channel
C
Artifact
B
A

Figure 6B

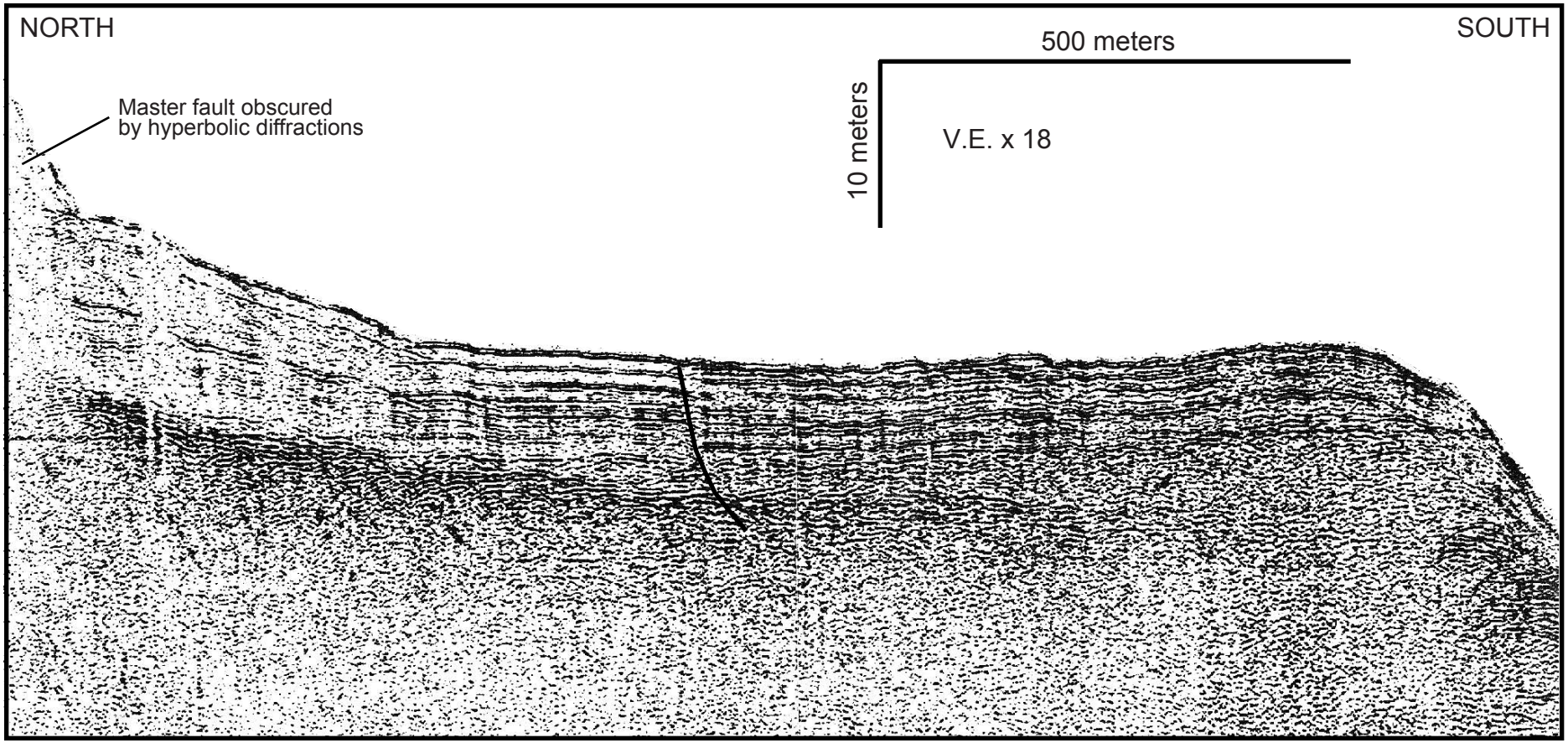
NORTH
SOUTH
500 meters
10 meters
V.E. x 18
Master fault obscured
by hyperbolic diffractions

Figure 6C

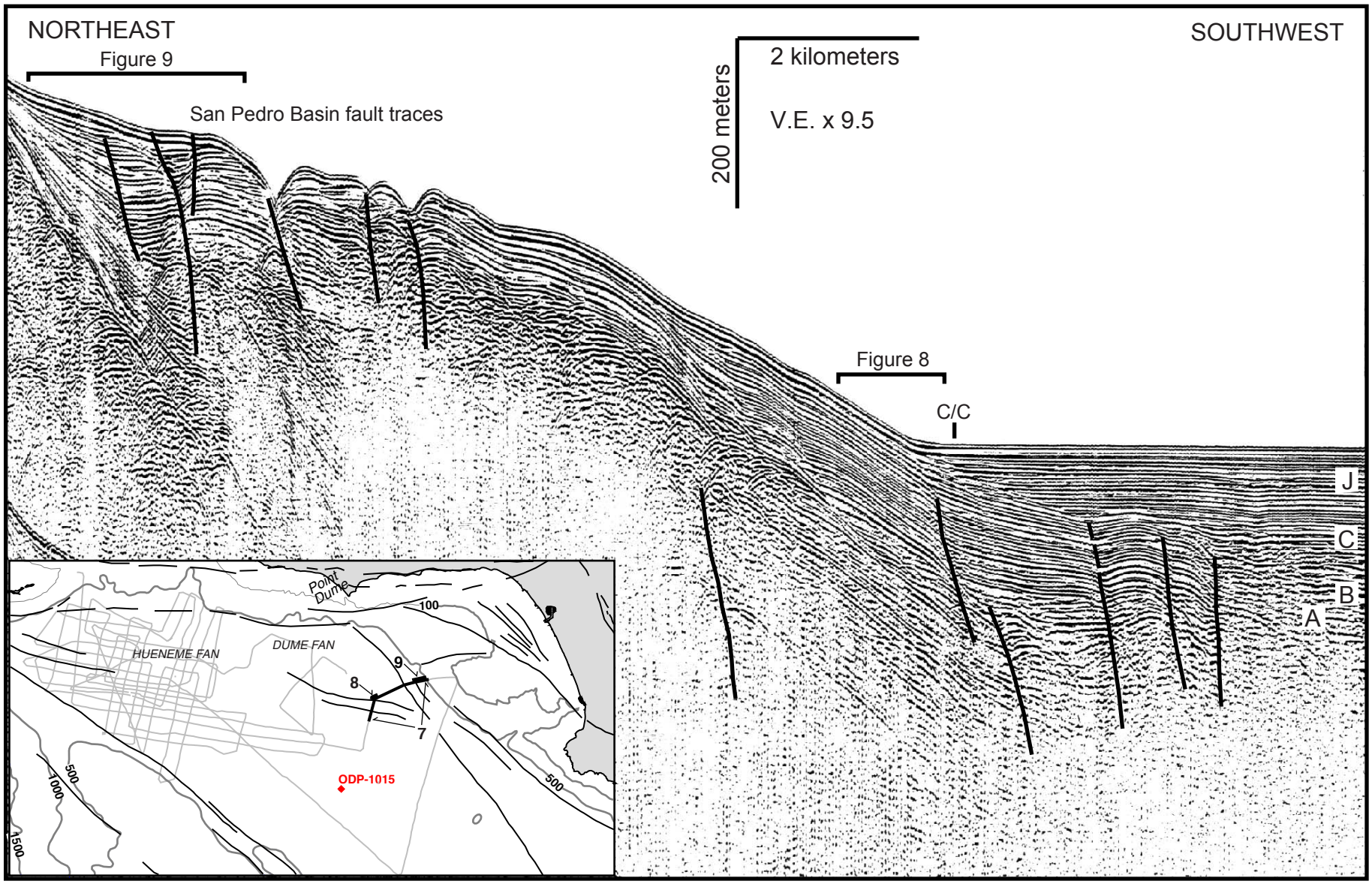
NORTHEAST
SOUTHWEST
Figure 9
San Pedro Basin fault traces
2 kilometers
V.E. x 9.5
200 meters
Figure 8
C/C
J
C
B
A
Point Dume
HUENEME FAN
DUME FAN
100
9
8
7
ODP-1015
500
1000
1500
500

Figure 7

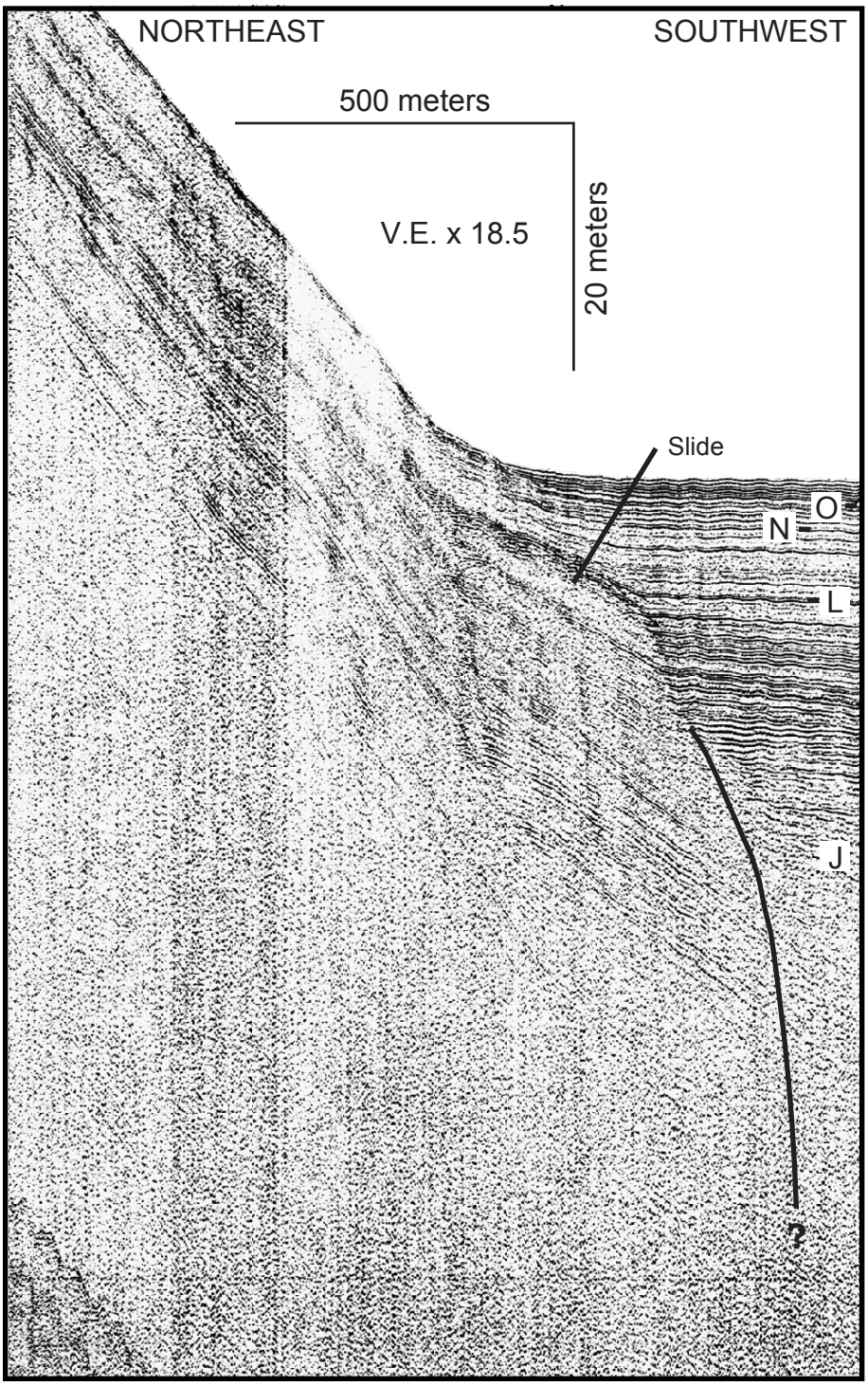
NORTHEAST
SOUTHWEST
500 meters
V.E. x 18.5
20 meters
Slide
O
N
L
J
?

Figure 8

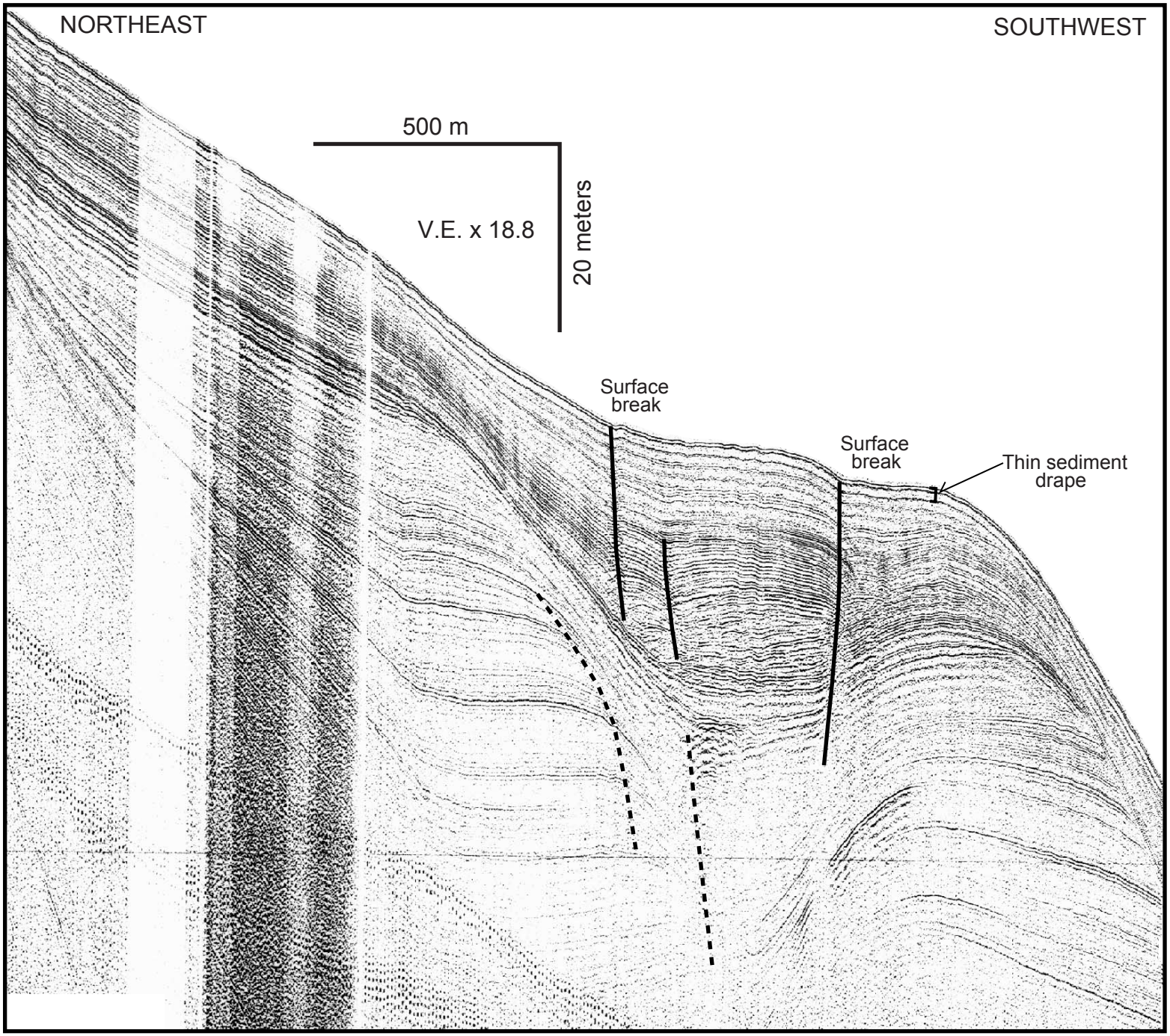
NORTHEAST
SOUTHWEST
500 m
V.E. x 18.8
20 meters
Surface break
Surface break
Thin sediment drape

Figure 9

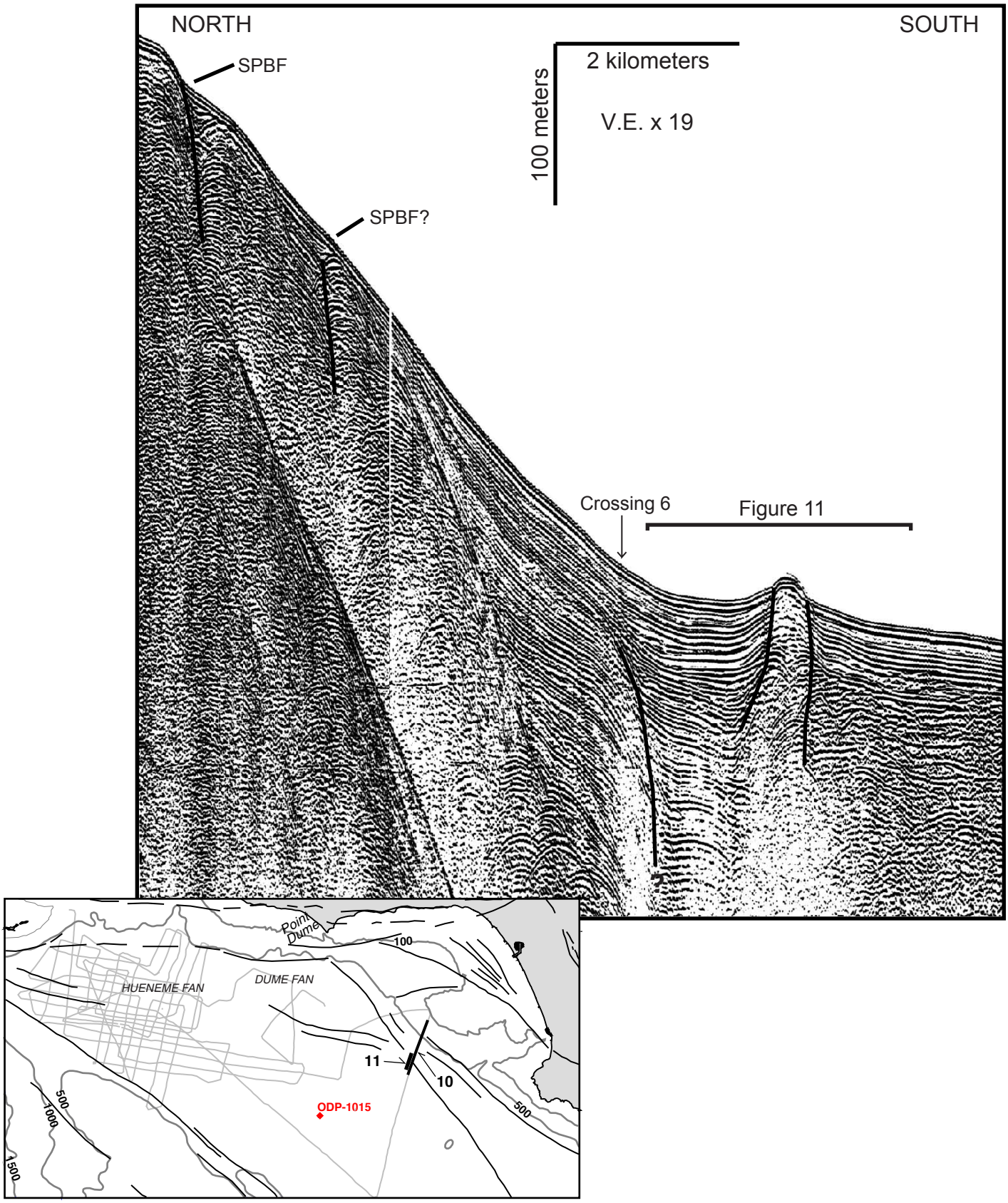
NORTH
SOUTH
SPBF
SPBF?
2 kilometers
100 meters
V.E. x 19
Crossing 6
Figure 11
Point Dume
100
HUENEME FAN
DUME FAN
11
10
ODP-1015
500
1000
1500
500

Figure 10

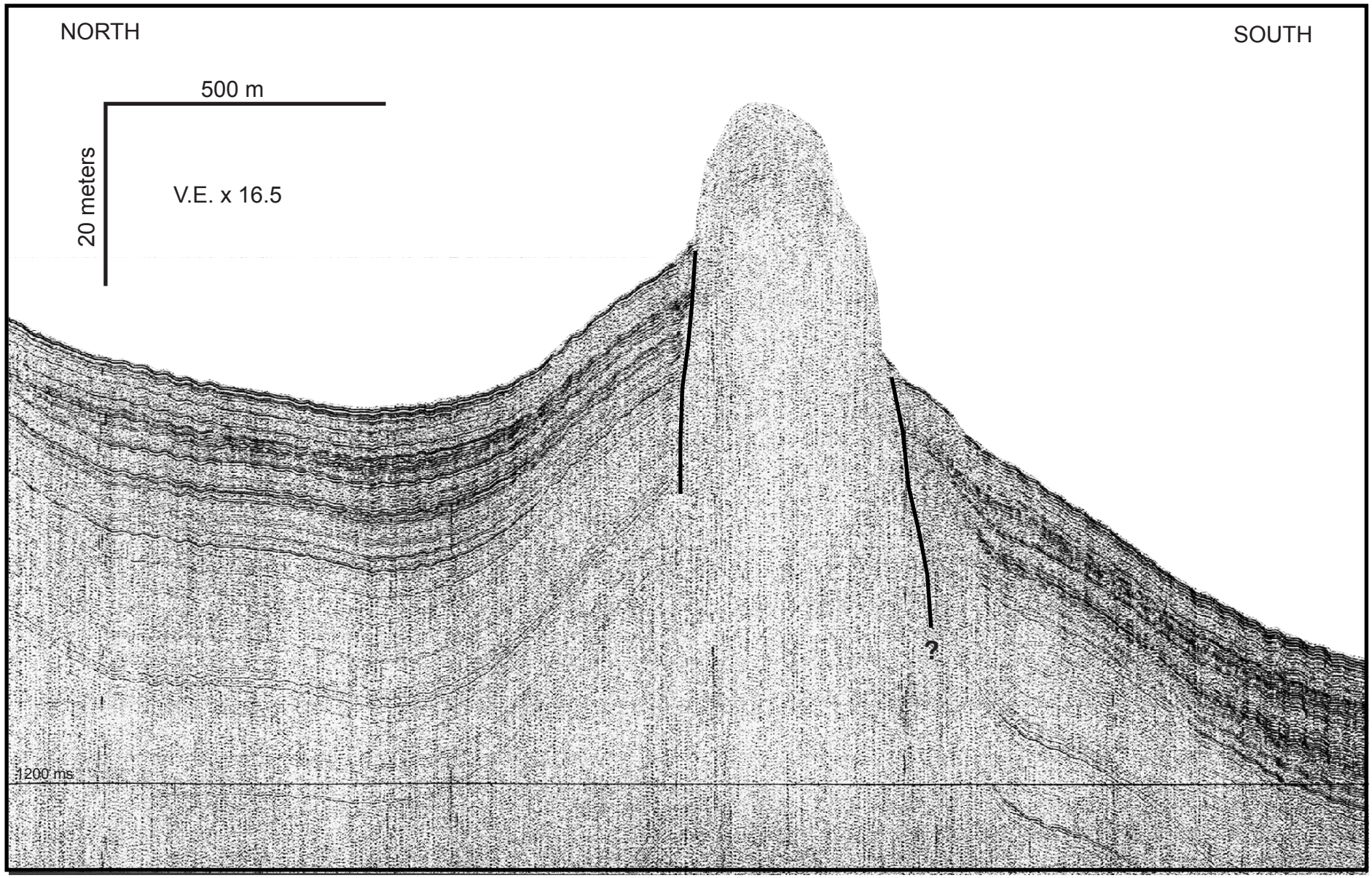

Figure 11

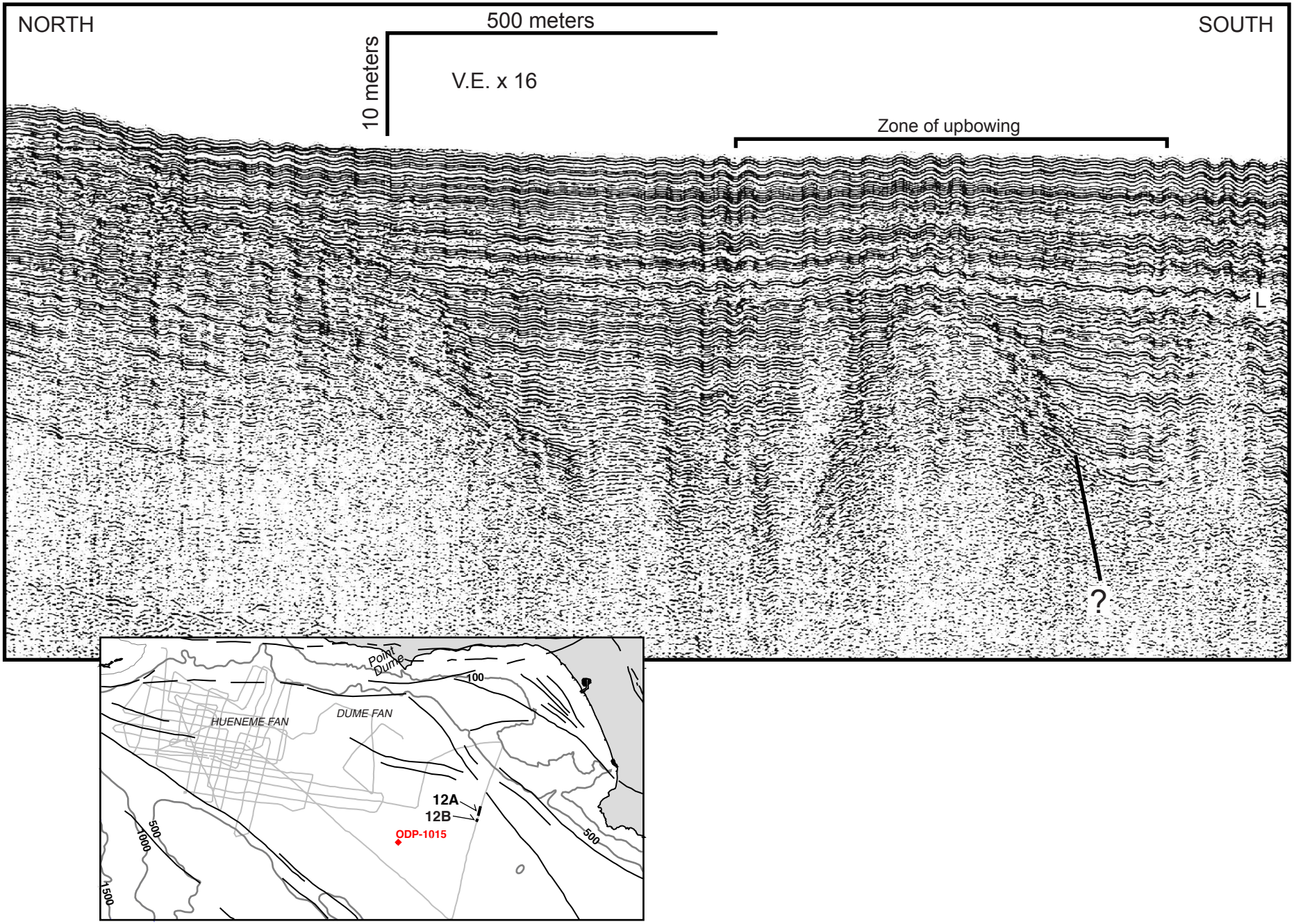
NORTH
500 meters
SOUTH
10 meters
V.E. x 16
Zone of upbowing
L
?
Point Dume
100
HUENEME FAN
DUME FAN
12A
12B
ODP-1015
500
1000
1500
500

Figure 12A

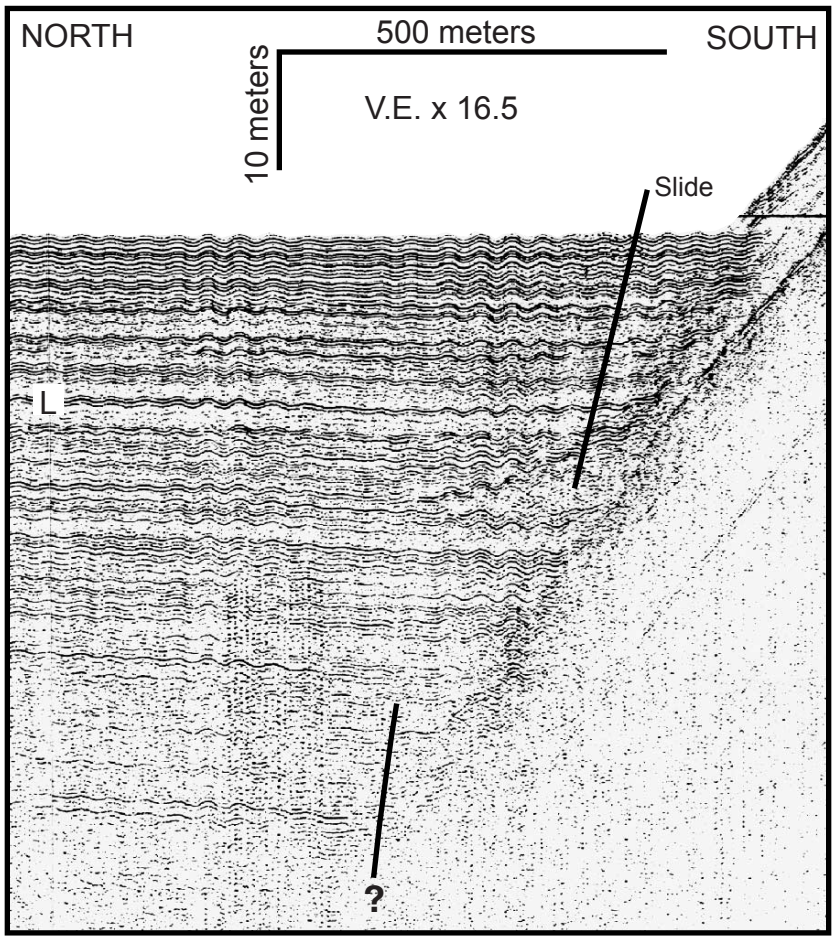

Figure 12B

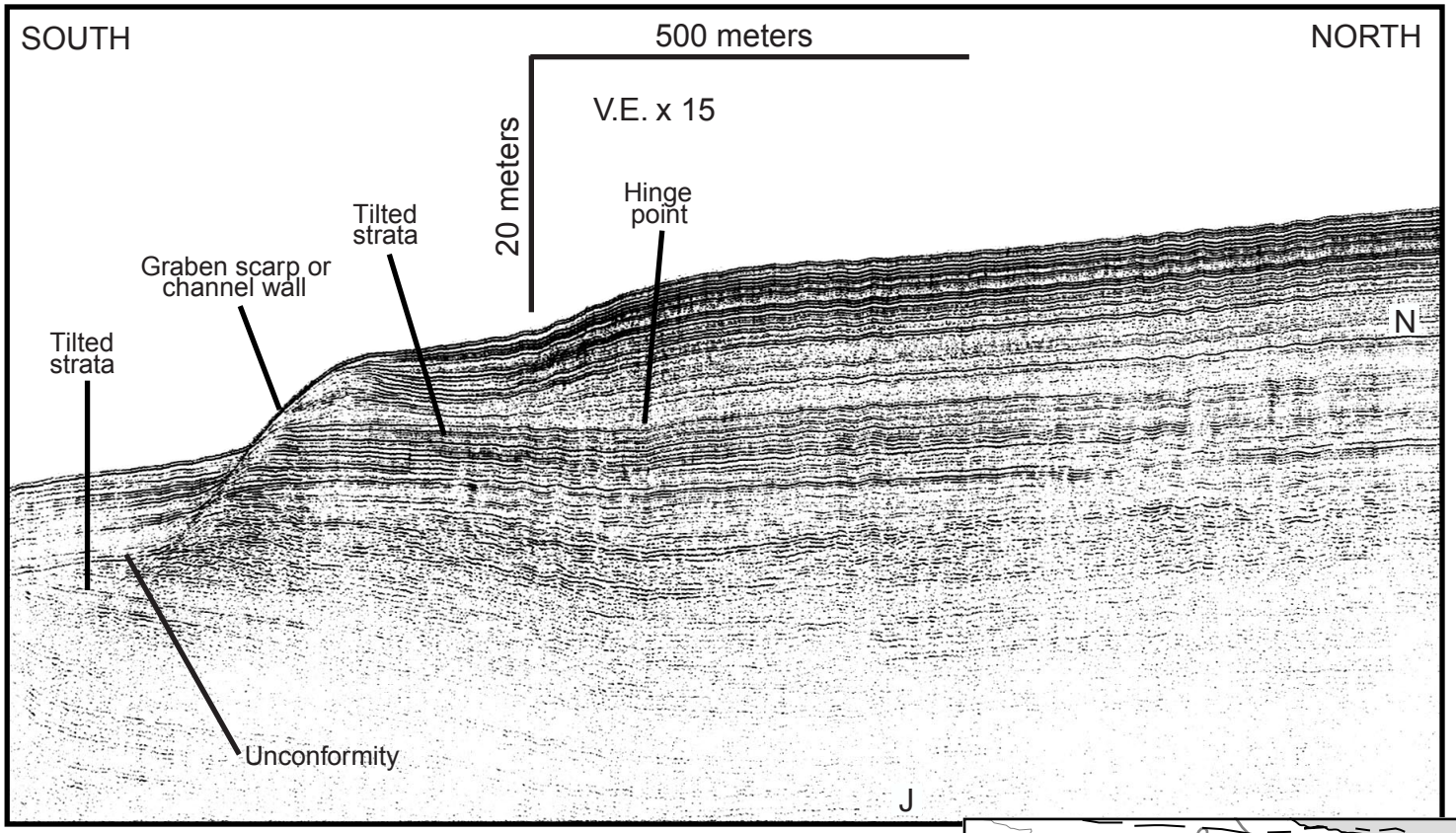
SOUTH
500 meters
NORTH
V.E. x 15
20 meters
Hinge point
Tilted strata
Graben scarp or channel wall
Tilted strata
N
Unconformity
J

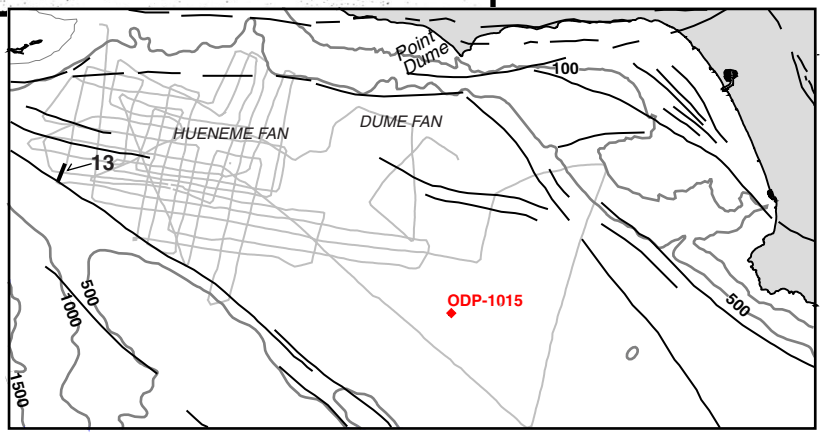
Point Dume
100
HUENEME FAN
DUME FAN
13
ODP-1015
500
1000
1500
500

Figure 13

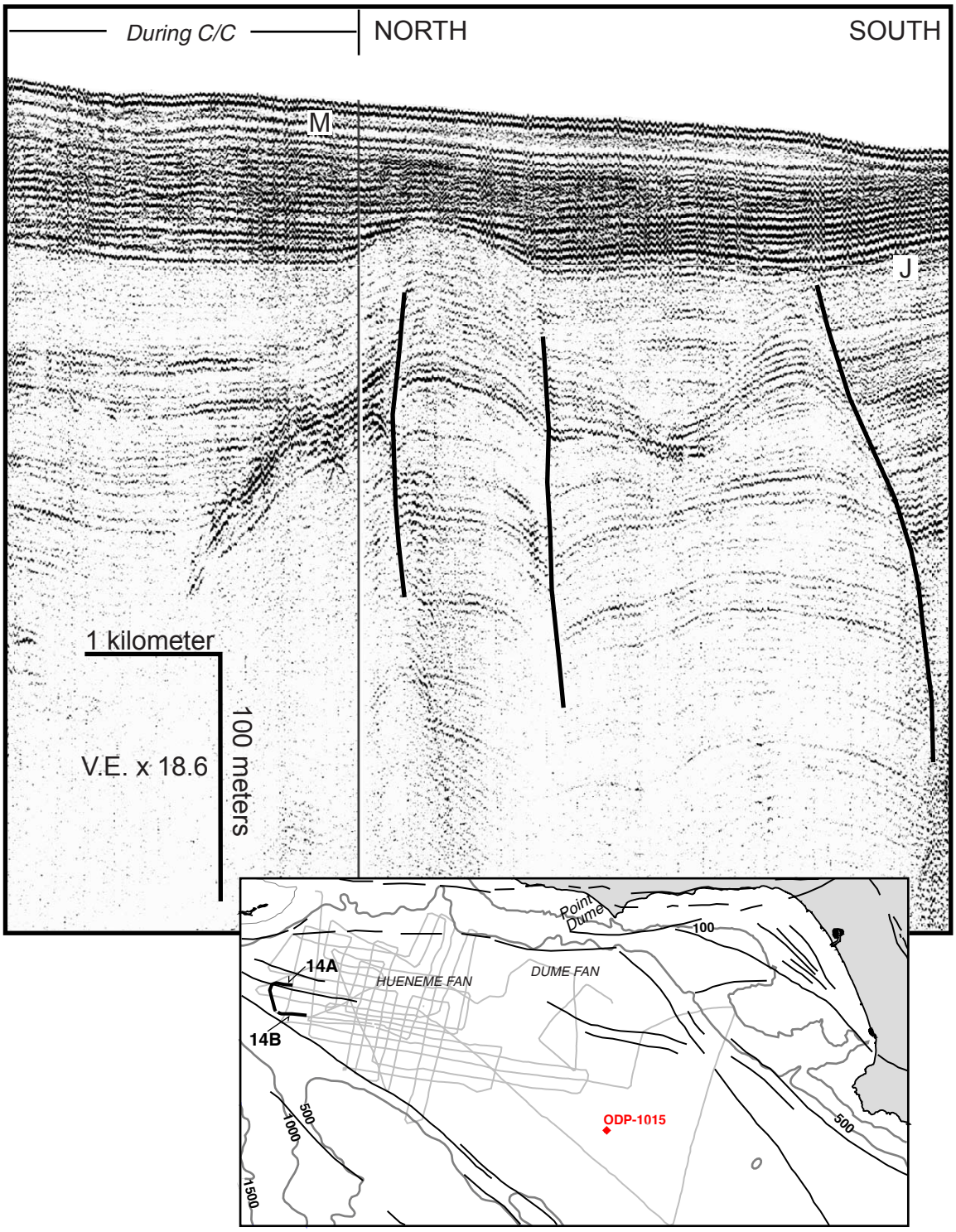
During C/C
NORTH
SOUTH
M
J
1 kilometer
V.E. x 18.6
100 meters
Point Dume
100
14A
HUENEME FAN
DUME FAN
14B
ODP-1015
500
1000
1500
500

Figure 14A

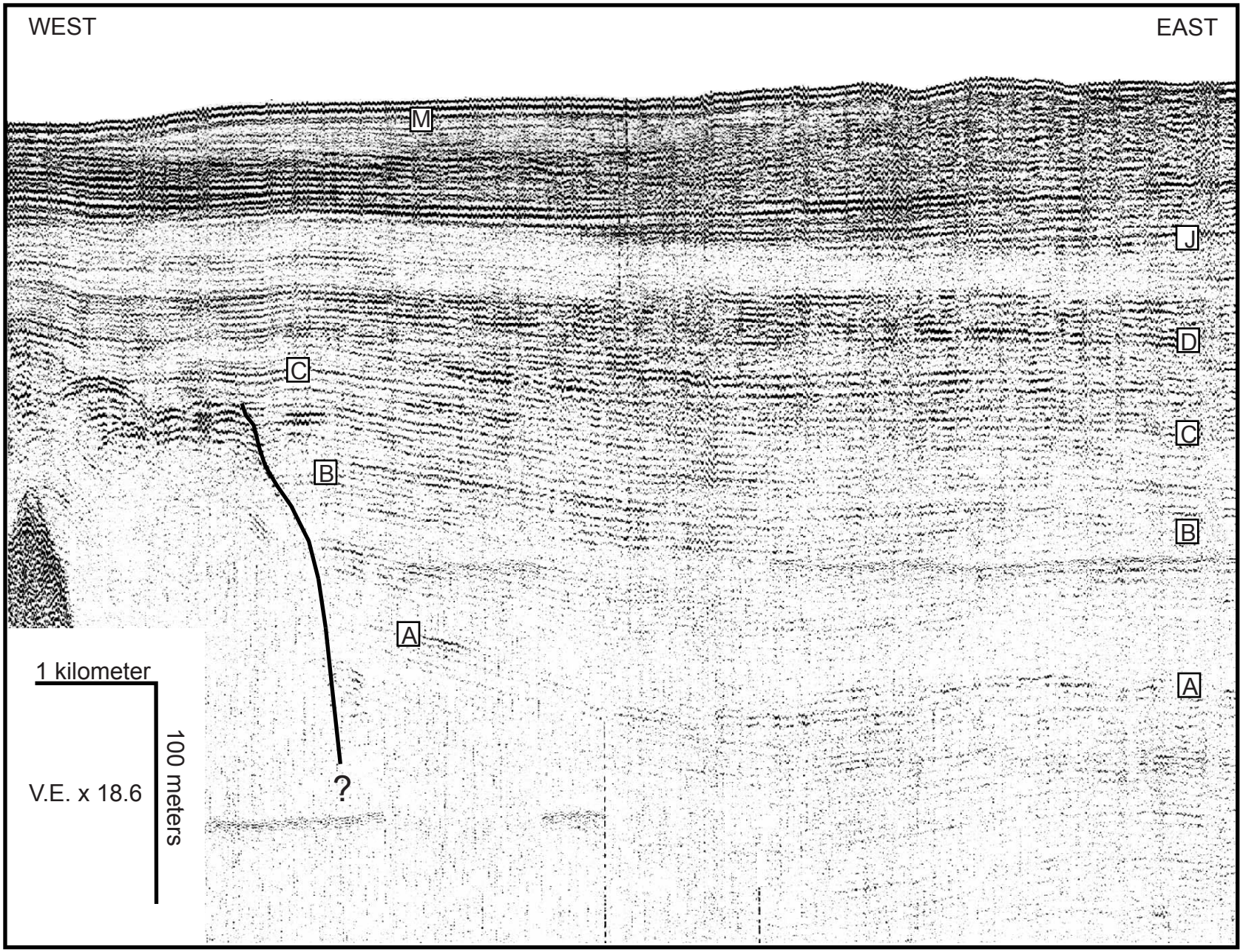

Figure 14B

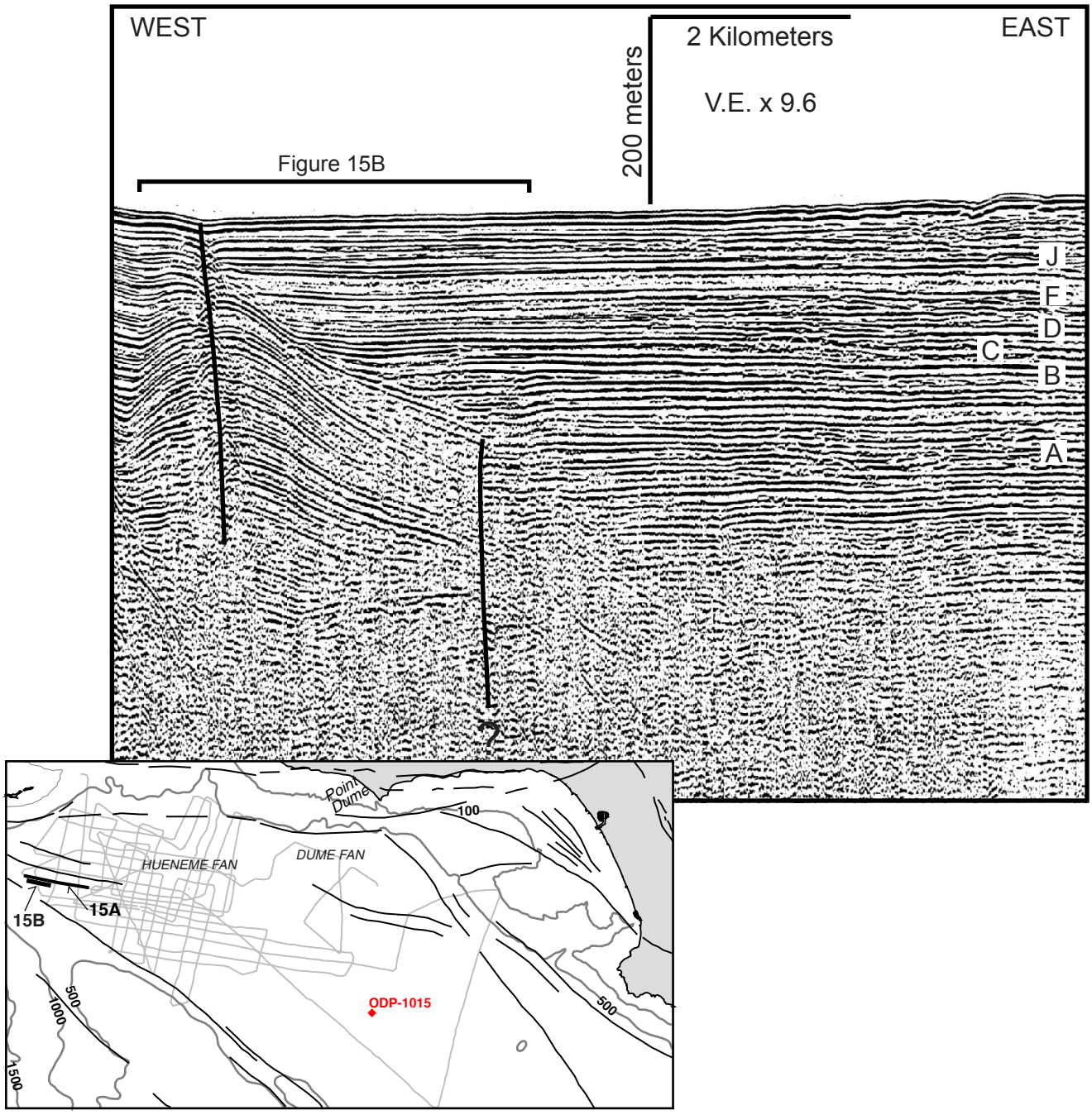
WEST
EAST
2 Kilometers
200 meters
V.E. x 9.6
Figure 15B
J
F
D
C
B
A
?
Point Dume
100
HUENEME FAN
DUME FAN
15B
15A
ODP-1015
500
1000
1500
500

Figure 15A

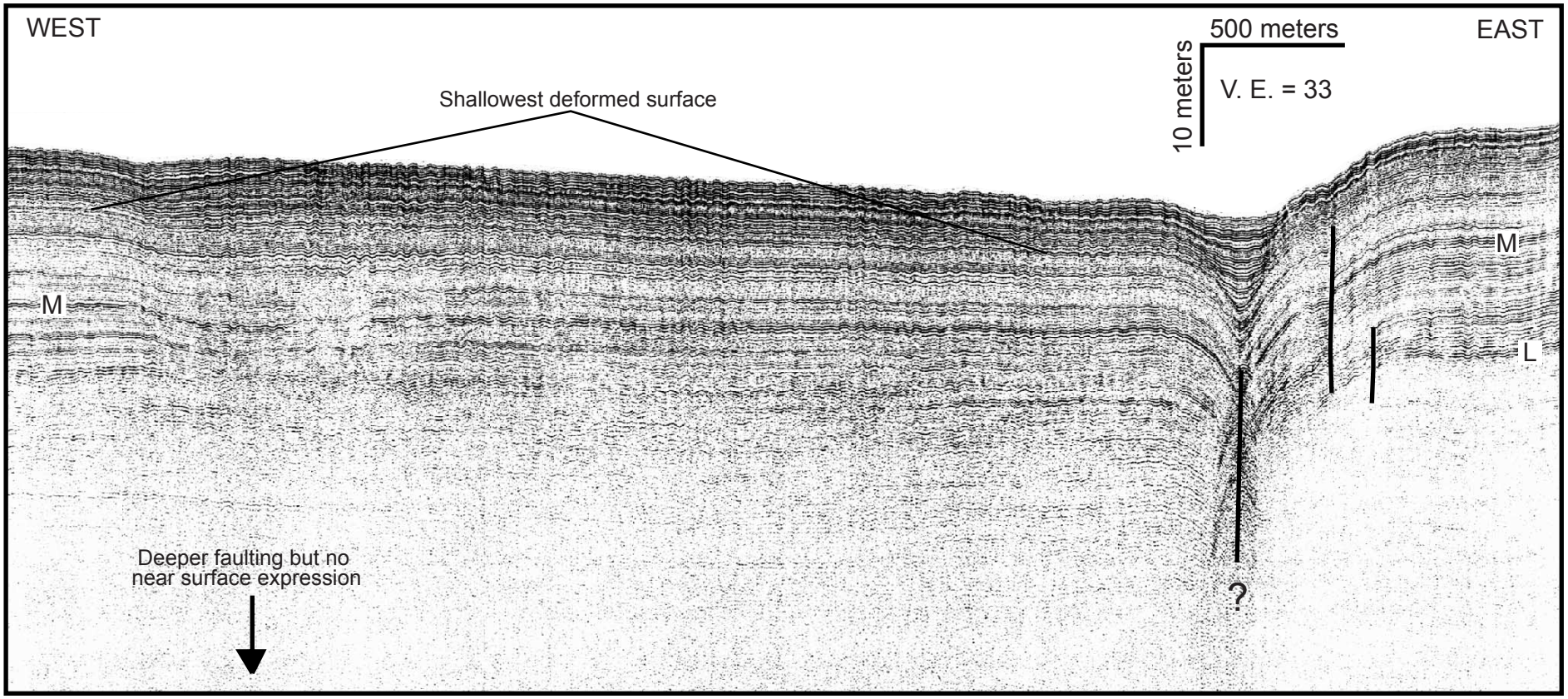
WEST
500 meters
EAST
10 meters
V. E. = 33
Shallowest deformed surface
M
M
L
Deeper faulting but no
near surface expression
?

Figure 15B

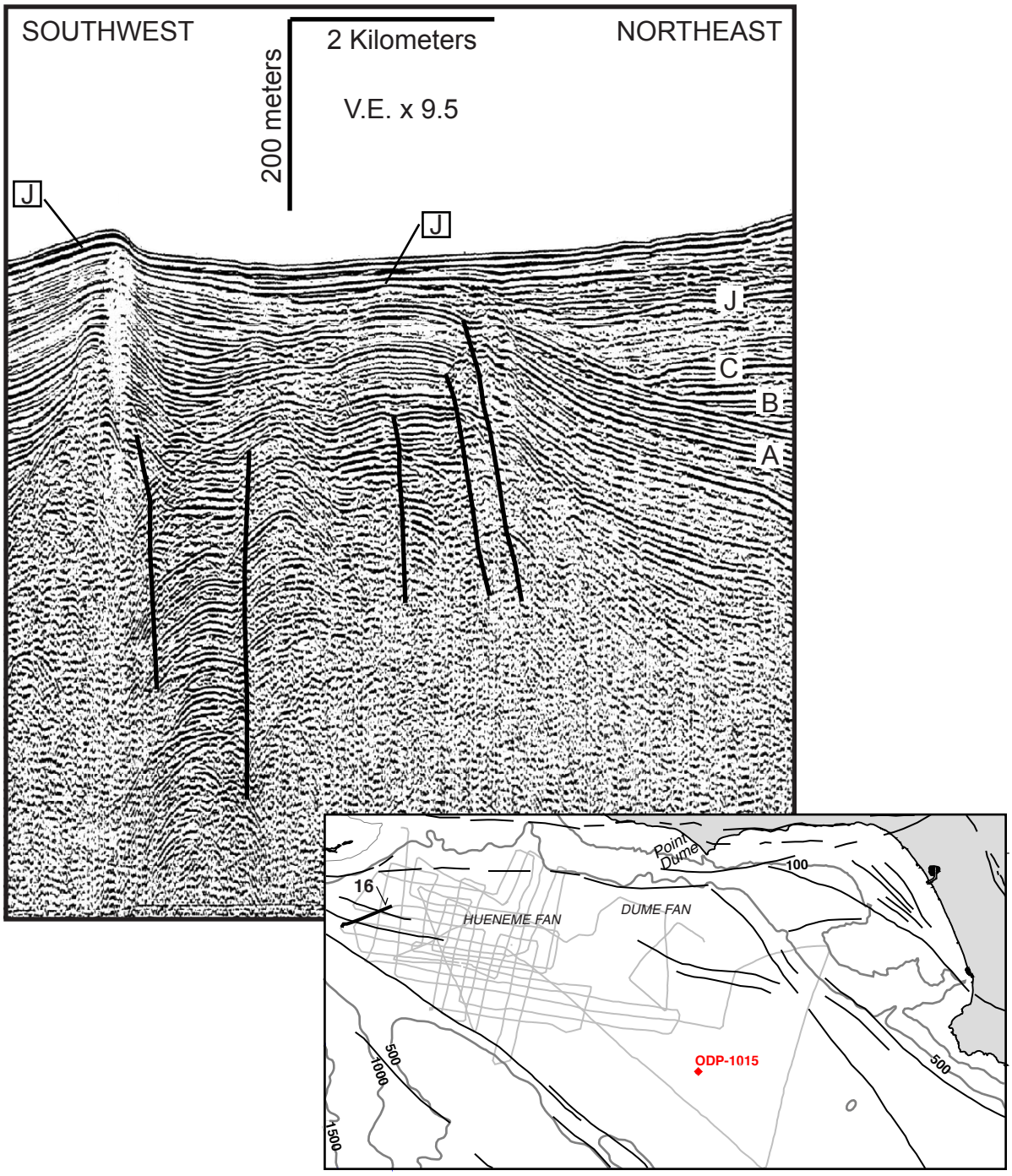
SOUTHWEST
NORTHEAST
2 Kilometers
200 meters
V.E. x 9.5
J
J
J
C
B
A
Point Dume
100
16
HUENEME FAN
DUME FAN
ODP-1015
500
1000
1500
500

Figure 16

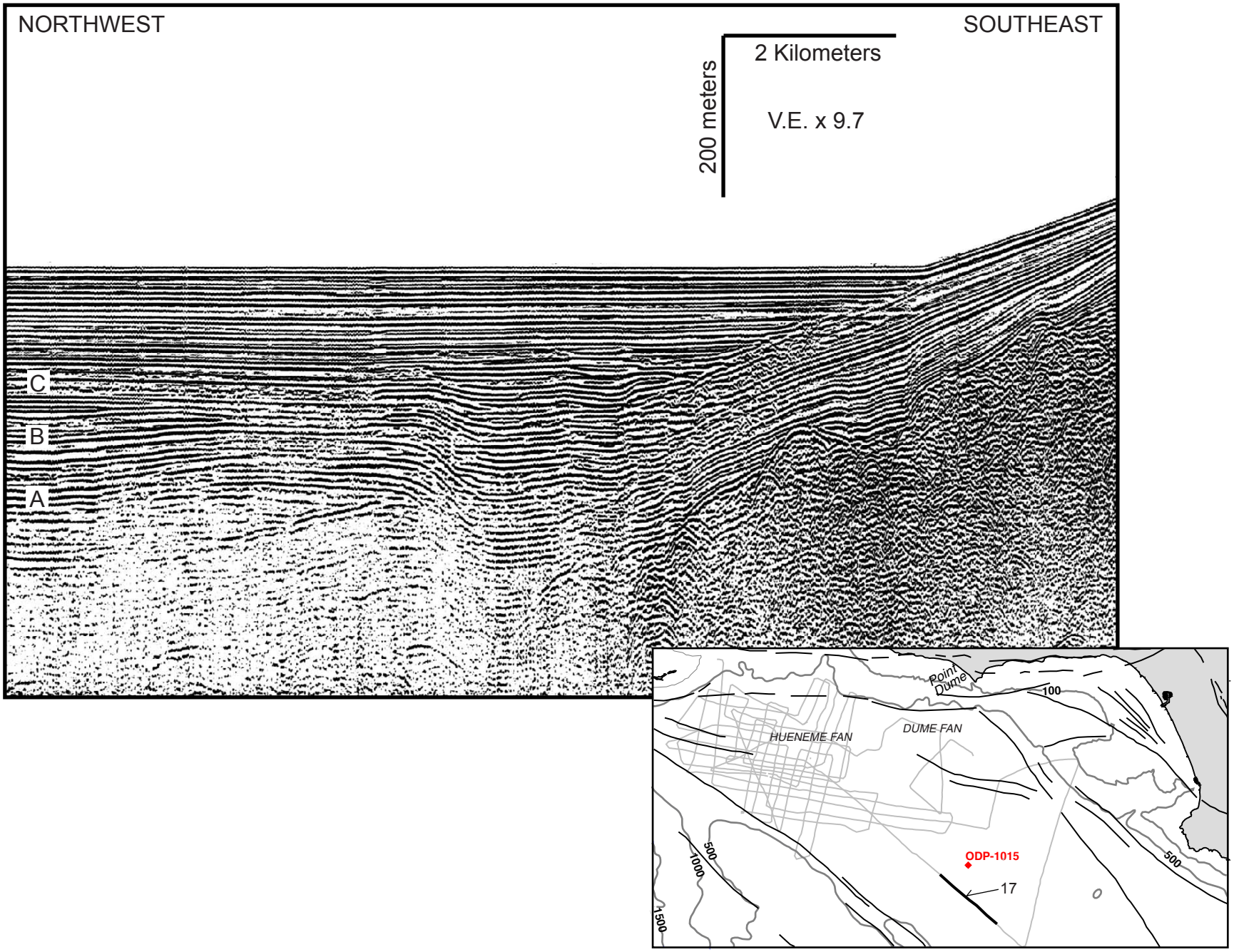
NORTHWEST
SOUTHEAST
2 Kilometers
200 meters
V.E. x 9.7
C
B
A
Point Dume
100
HUENEME FAN
DUME FAN
500
1000
1500
ODP-1015
17
500

Figure 17

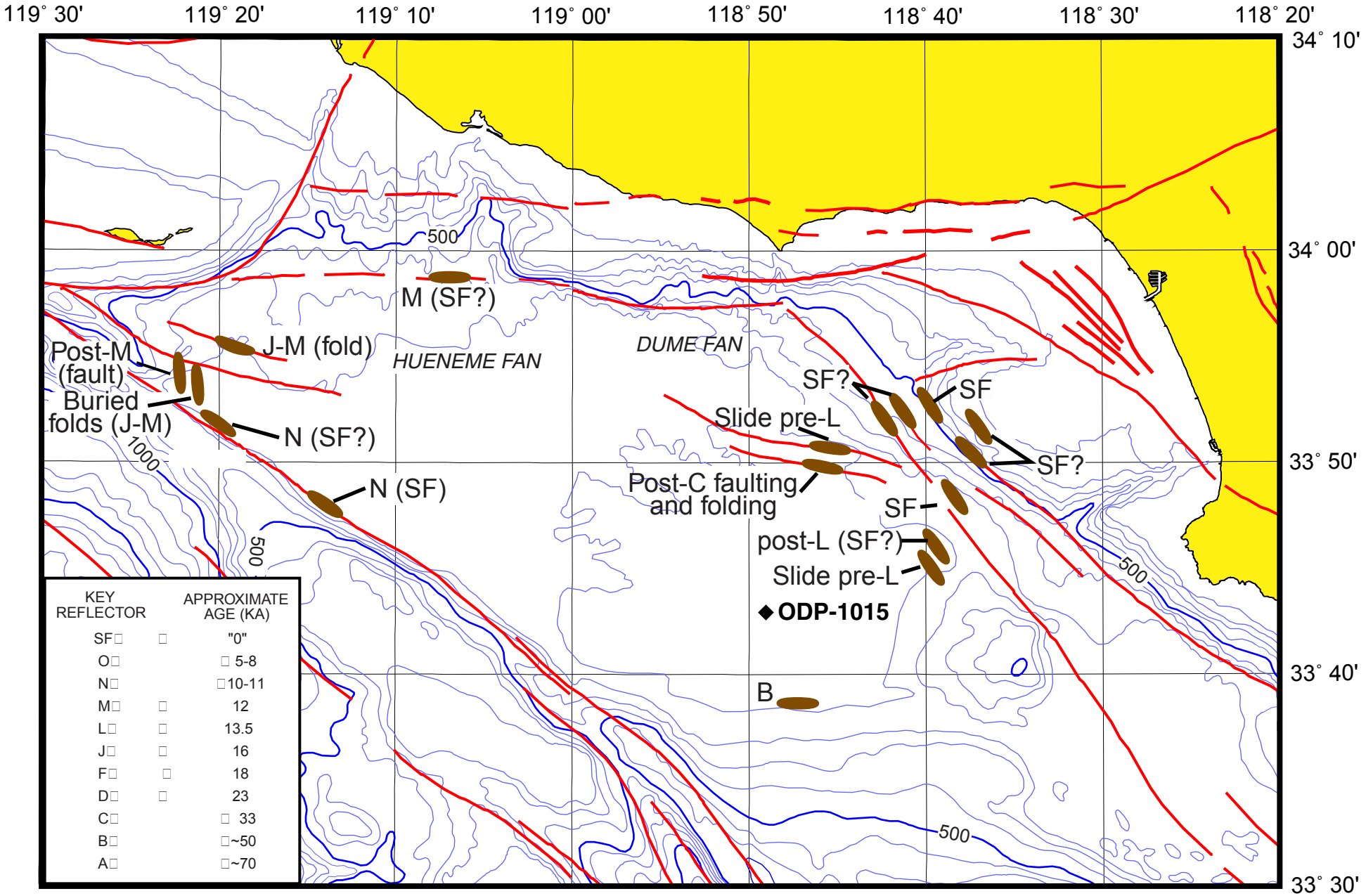
119° 30'
119° 20'
119° 10'
119° 00'
118° 50'
118° 40'
118° 30'
118° 20'
34° 10'
34° 00'
33° 50'
33° 40'
33° 30'
500
M (SF?)
J-M (fold)
HUENEME FAN
DUME FAN
Post-M (fault)
Buried folds (J-M)
N (SF?)
1000
N (SF)
500
SF?
SF
Slide pre-L
SF?
Post-C faulting and folding
SF
post-L (SF?)
Slide pre-L
◆ ODP-1015
500
B
500
KEY REFLECTOR
APPROXIMATE AGE (KA)
SF
"0"
O
5-8
N
10-11
M
12
L
13.5
J
16
F
18
D
23
C
33
B
~50
A
~70

Figure 18

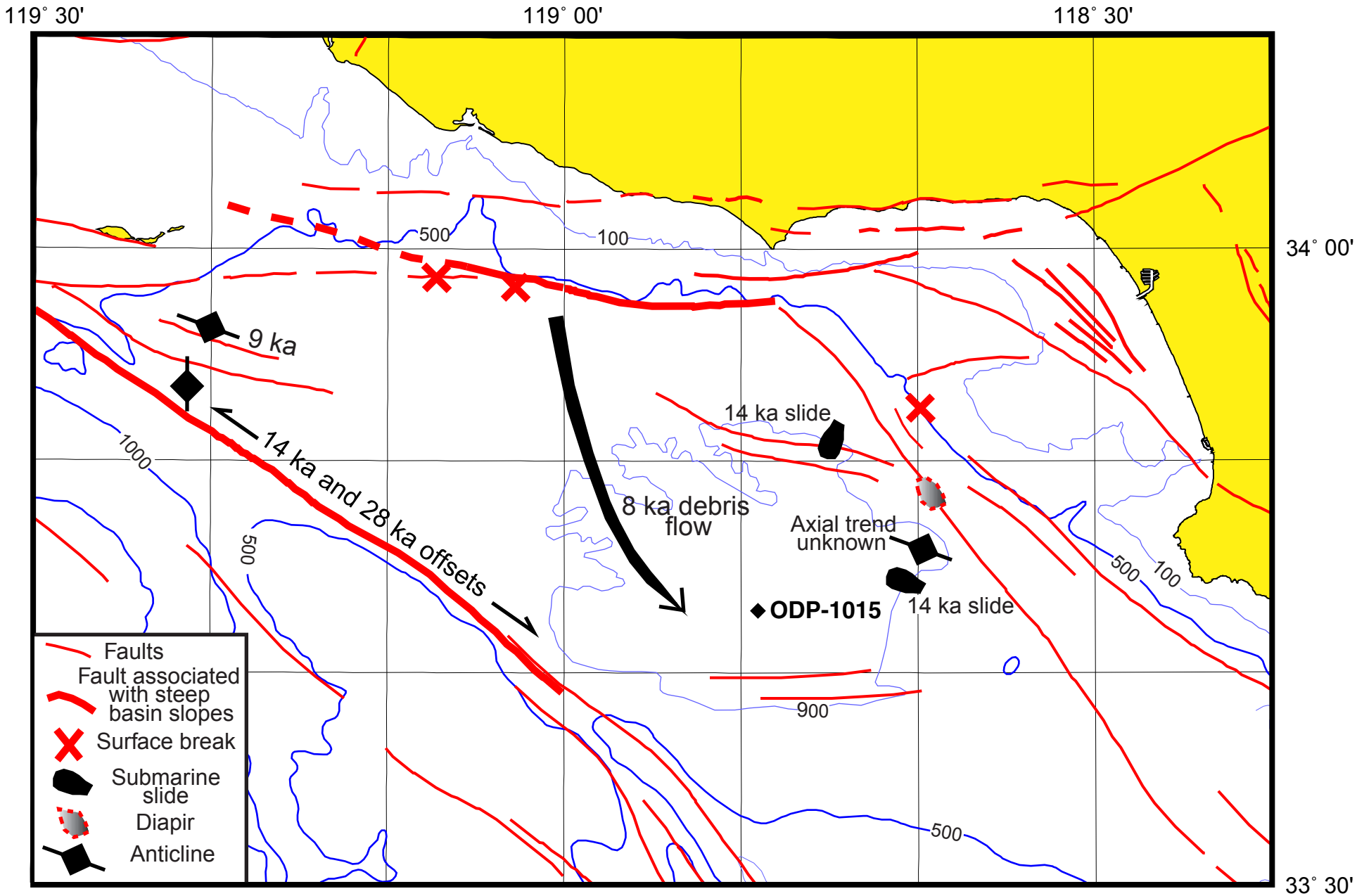
119° 30'
119° 00'
118° 30'
34° 00'
33° 30'
500
100
9 ka
14 ka and 28 ka offsets
1000
500
14 ka slide
8 ka debris flow
Axial trend unknown
ODP-1015
14 ka slide
500
100
900
500
Faults
Fault associated with steep basin slopes
Surface break
Submarine slide
Diapir
Anticline

Figure 19